Revealing Subtle Active Tectonic Deformation: Integrating Lidar, Photogrammetry, Field Mapping, and Geophysical Surveys to Assess the Late Quaternary Activity of the Sava Fault (Southern Alps, Slovenia) - Supplementary Materials

Petra Jamšek Rupnik 1,*, Jure Atanackov 1, Barbara Horn 2,3, Branko Mušič 2,3, Marjana Zajc 1, Christoph Grützner 4, Kamil Ustaszewski 4, Sumiko Tsukamoto 5,6, Matevž Novak 1, Blaž Milanič 1, Anže Markelj 1, Kristina Ivančič 1, Ana Novak 1, Jernej Jež 1, Manja Žebre 1, Miloš Bavec 1 and Marko Vrabec 7

1 Geological Survey of Slovenia, Dimičeva ul. 14, 1000 Ljubljana, Slovenia; jure.atanackov@geo-zs.si (J.A.); marjana.zajc@geo-zs.si (M.Z.); matevz.novak@geo-zs.si (M.N.); blaz.milanic@geo-zs.si (B.M.); anze.markelj@geo-zs.si (A.M.); kristina.ivancic@geo-zs.si (K.I.); ana.novak@geo-zs.si (A.N.); jernej.jez@geo-zs.si (J.J.); manja.zebre@geo-zs.si (M.Ž.); milos.bavec@geo-zs.si (M.B.)

2 Department of Archeology, Faculty of Arts, University of Ljubljana, Aškerčeva c. 2, 1000 Ljubljana, Slovenia; barbarahorn01@gmail.com (B.H.); branko.music@ff.uni-lj.si (B.M.)

3 Gearh d.o.o., Radvanjska cesta 13, 2000 Maribor, Slovenia

4 Institute of Geosciences, Friedrich-Schiller-Universität Jena, Burgweg 11, 07749 Jena, Germany;

christoph.gruetzner@uni-jena.de (C.G.); kamil.u@uni-jena.de (K.U.)

5 Leibniz Institute for Applied Geophysics LIAG Hannover, Stilleweg 2, 30655 Hannover, Germany; sumiko.tsukamoto@leibniz-liag.de

6 Department of Geosciences, University of Tübingen, Schnarrenbergstr. 94–96, 72076 Tübingen, Germany

7 Department of Geology, Faculty of Natural Sciences and Engineering, University of Ljubljana, Aškerčeva c. 12, 1000 Ljubljana, Slovenia; marko.vrabec@ntf.uni-lj.si

* Correspondence: petra.jamsek@geo-zs.si

Section S1 – Digital Elevation Models

In this section we present uninterpreted Digital Elevation Models (DEMs) that we used for geomorphological mapping presented on Figures 2, 5 and 6 from the paper. DEMs are derived from lidar data [1] and photogrammetry. Different visual representations of the relief models were generated using QGIS and the Relief Visualization Toolbox plugin [2,3], including shaded relief, multidirectional shaded relief, slope map, aspect map, and Sky-View Factor (Figures S1-S14).

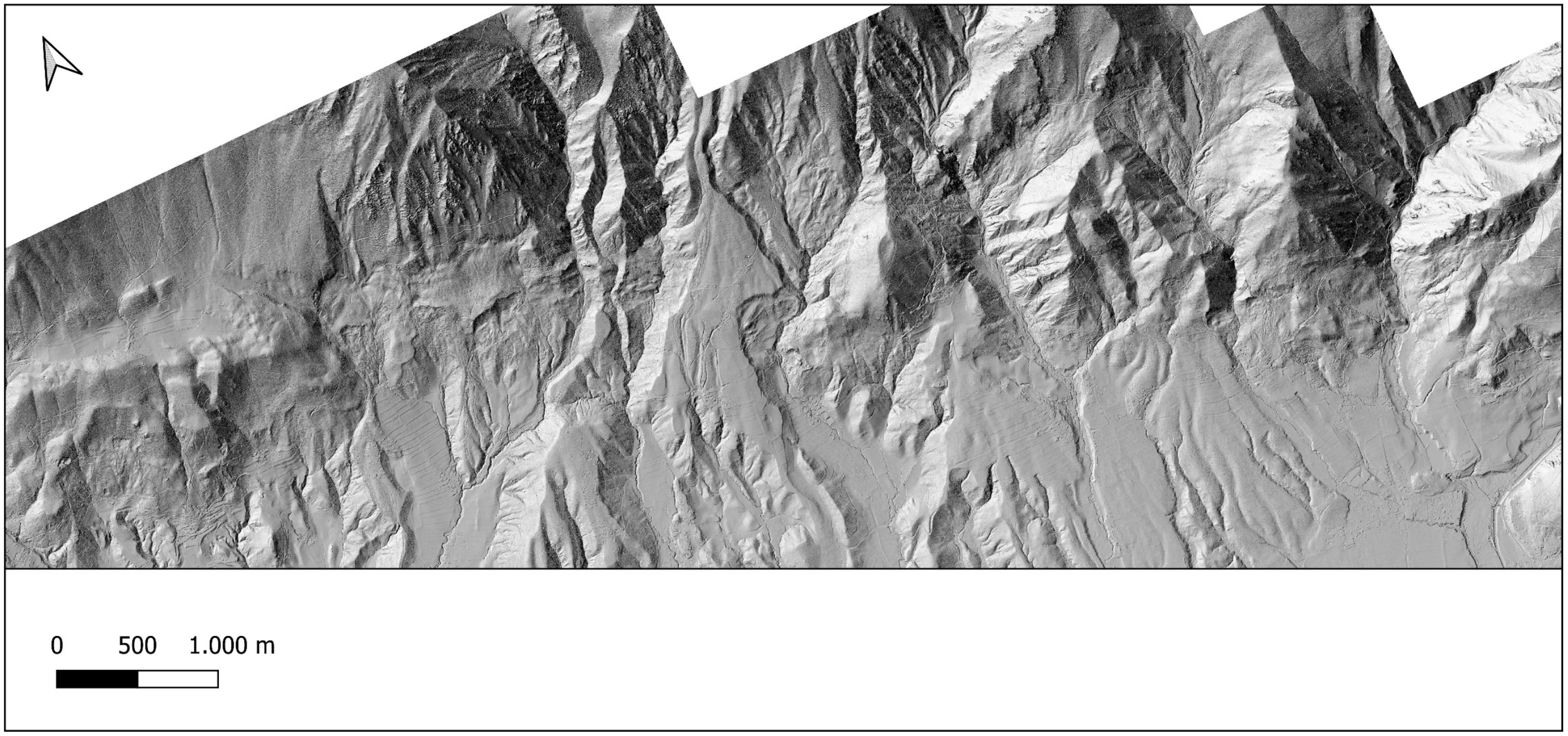

Figure S1: Shaded relief from lidar-derived DEM along the Sava Fault between Golnik and Preddvor.

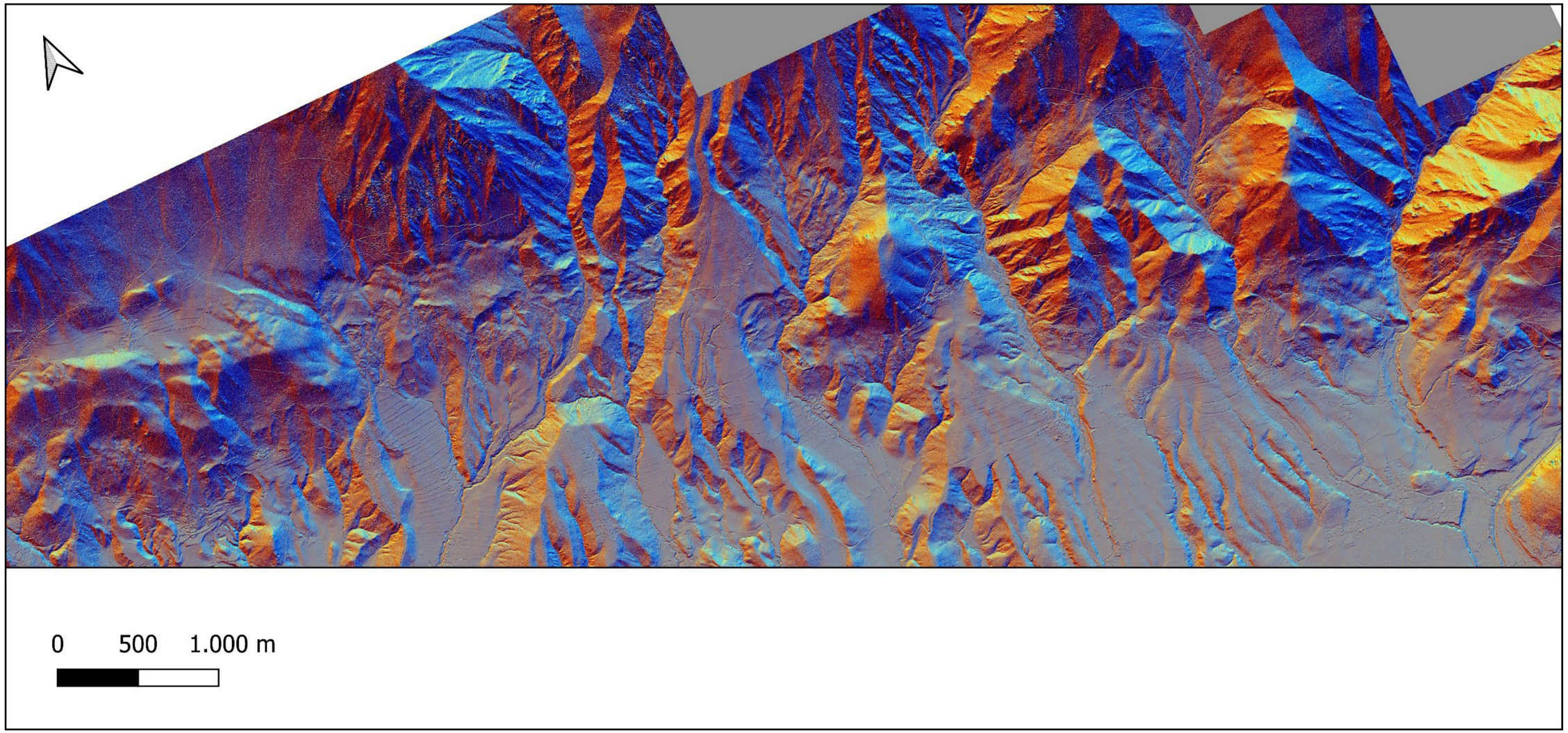

Figure S2: Multidirectional shaded relief from lidar-derived DEM along the Sava Fault between Golnik and Preddvor.

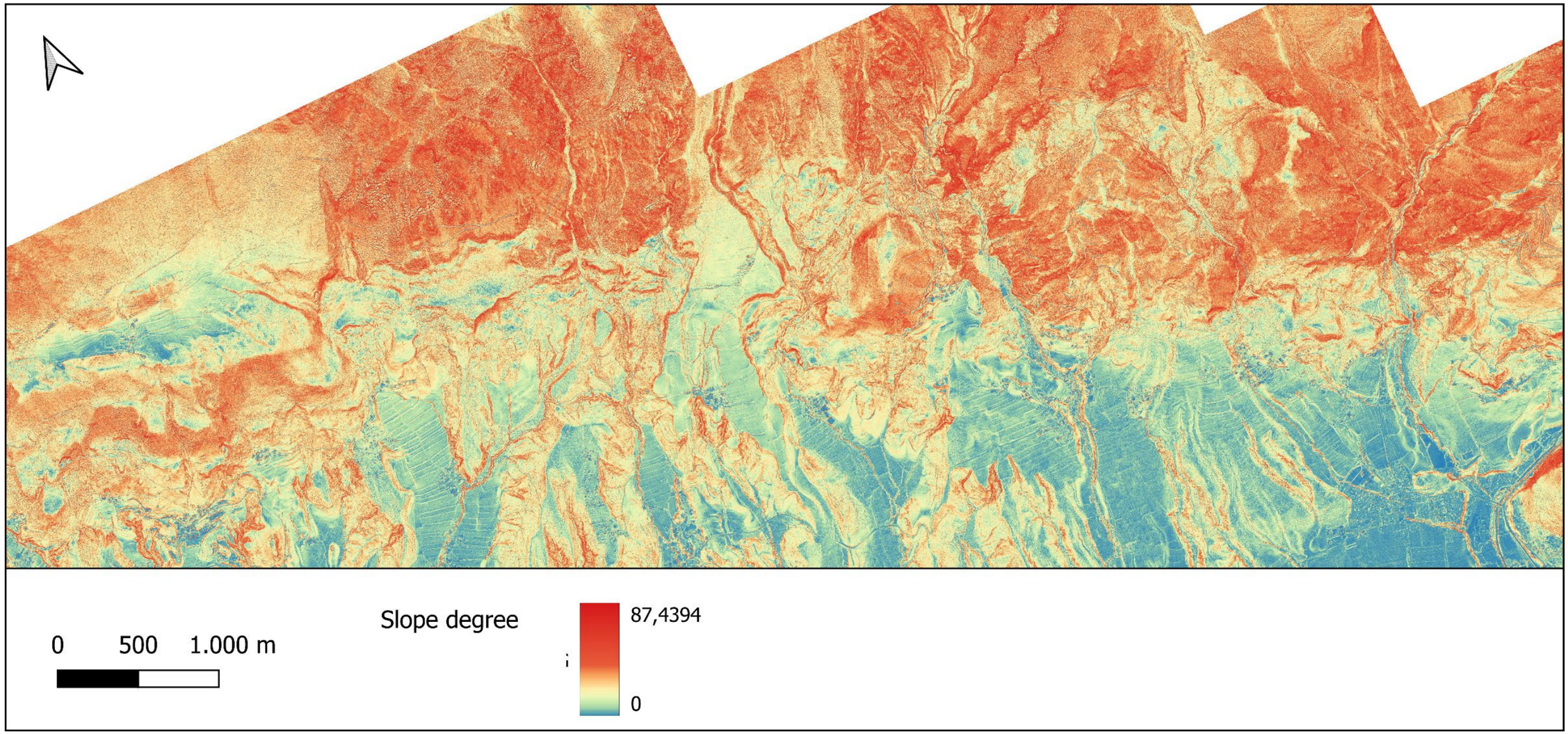

Figure S3: Slope map from lidar-derived DEM along the Sava Fault between Golnik and Preddvor.

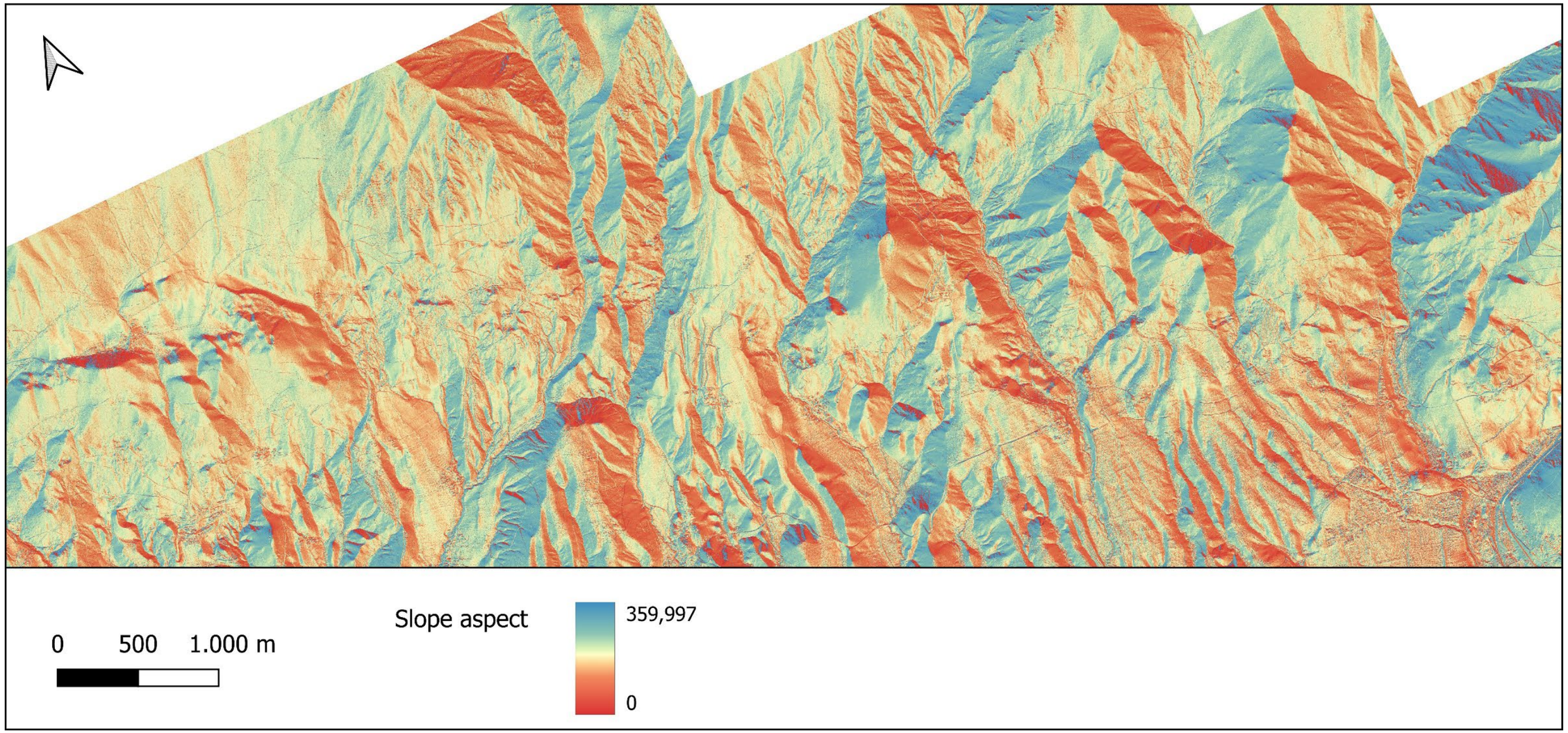

Figure S4: Aspect map from lidar-derived DEM along the Sava Fault between Golnik and Preddvor.

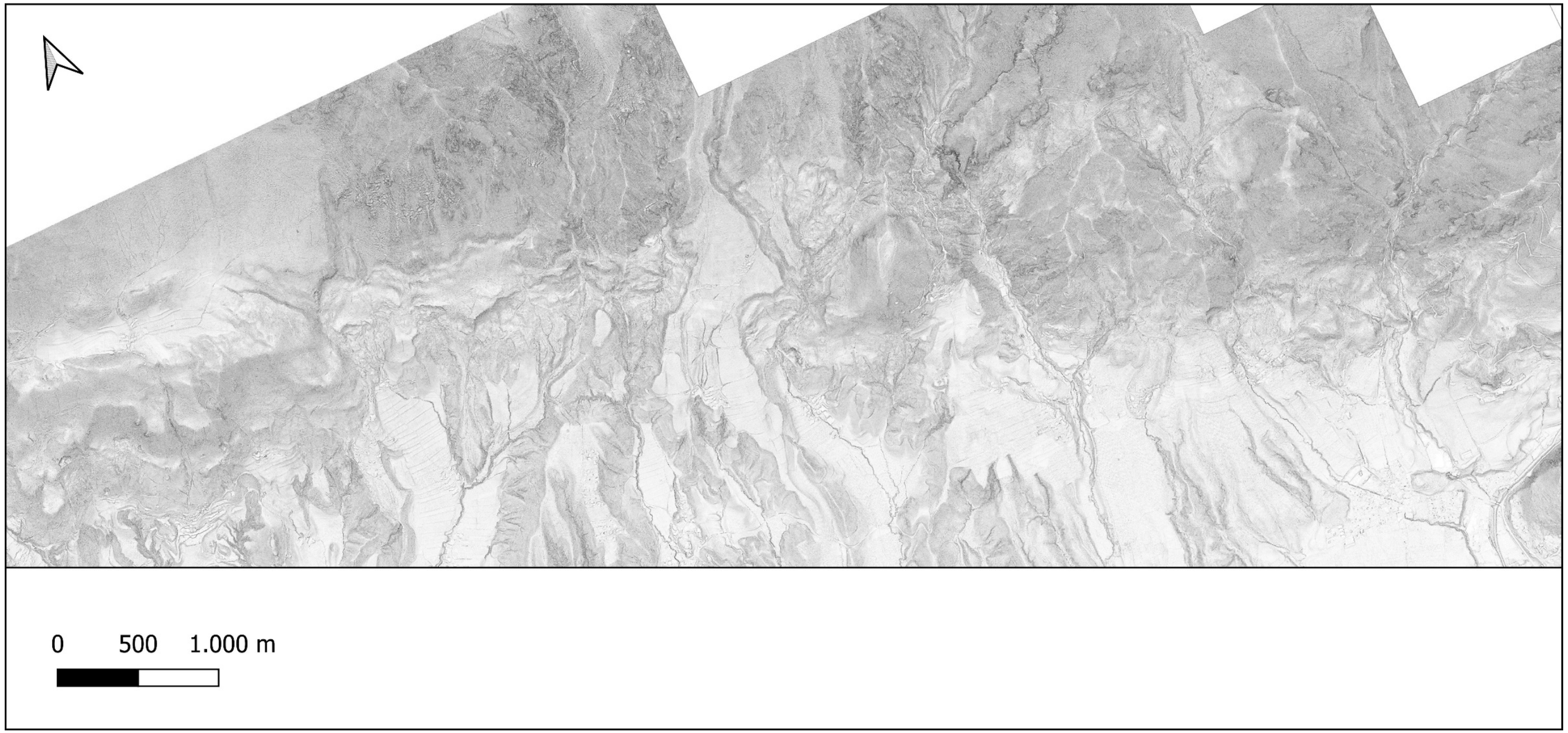

Figure S5: Sky View Factor visualization from lidar-derived DEM along the Sava Fault between Golnik and Preddvor.

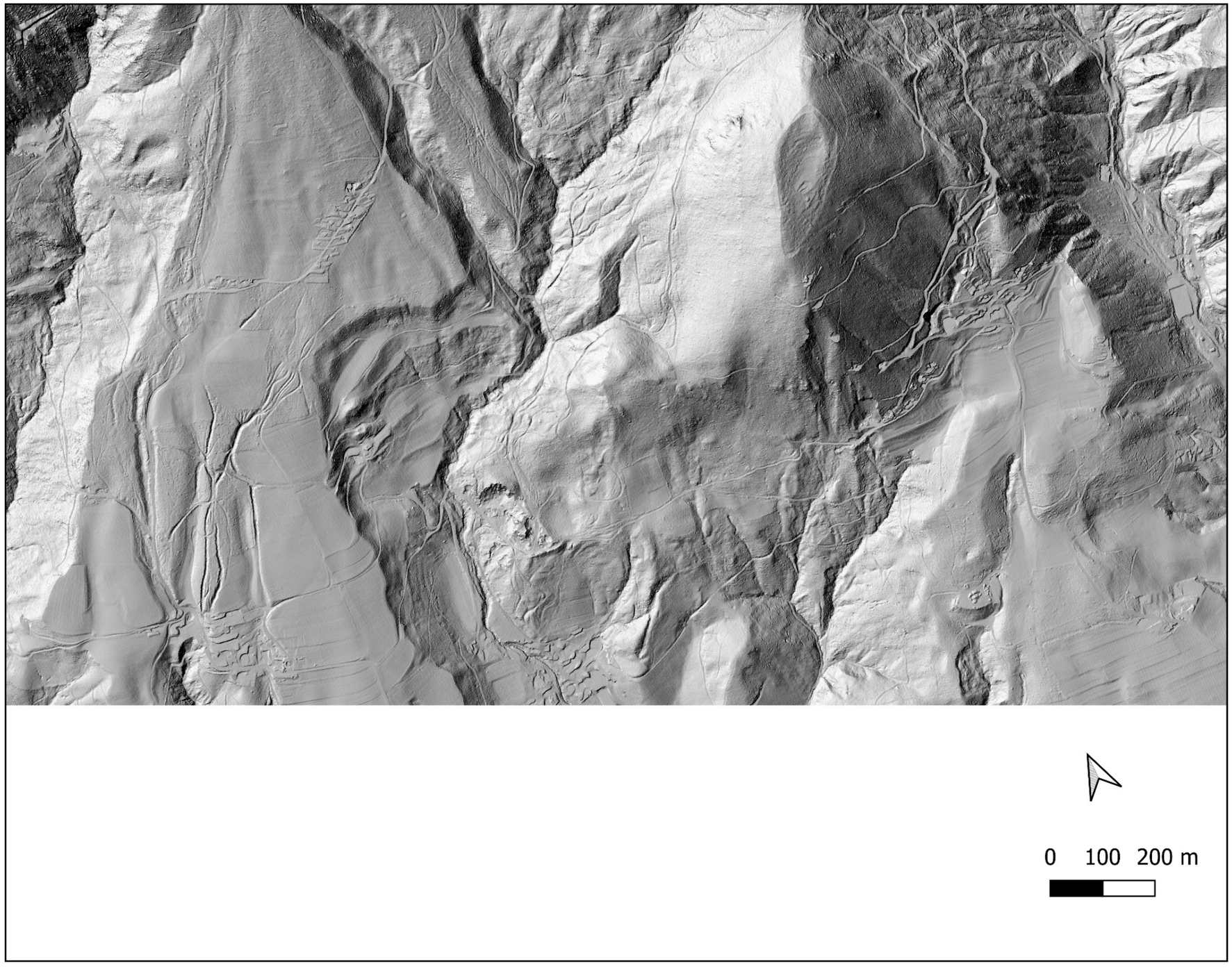

Figure S6: Shaded relief from lidar-derived DEM along the Sava Fault in the area of Povlje and Laško.

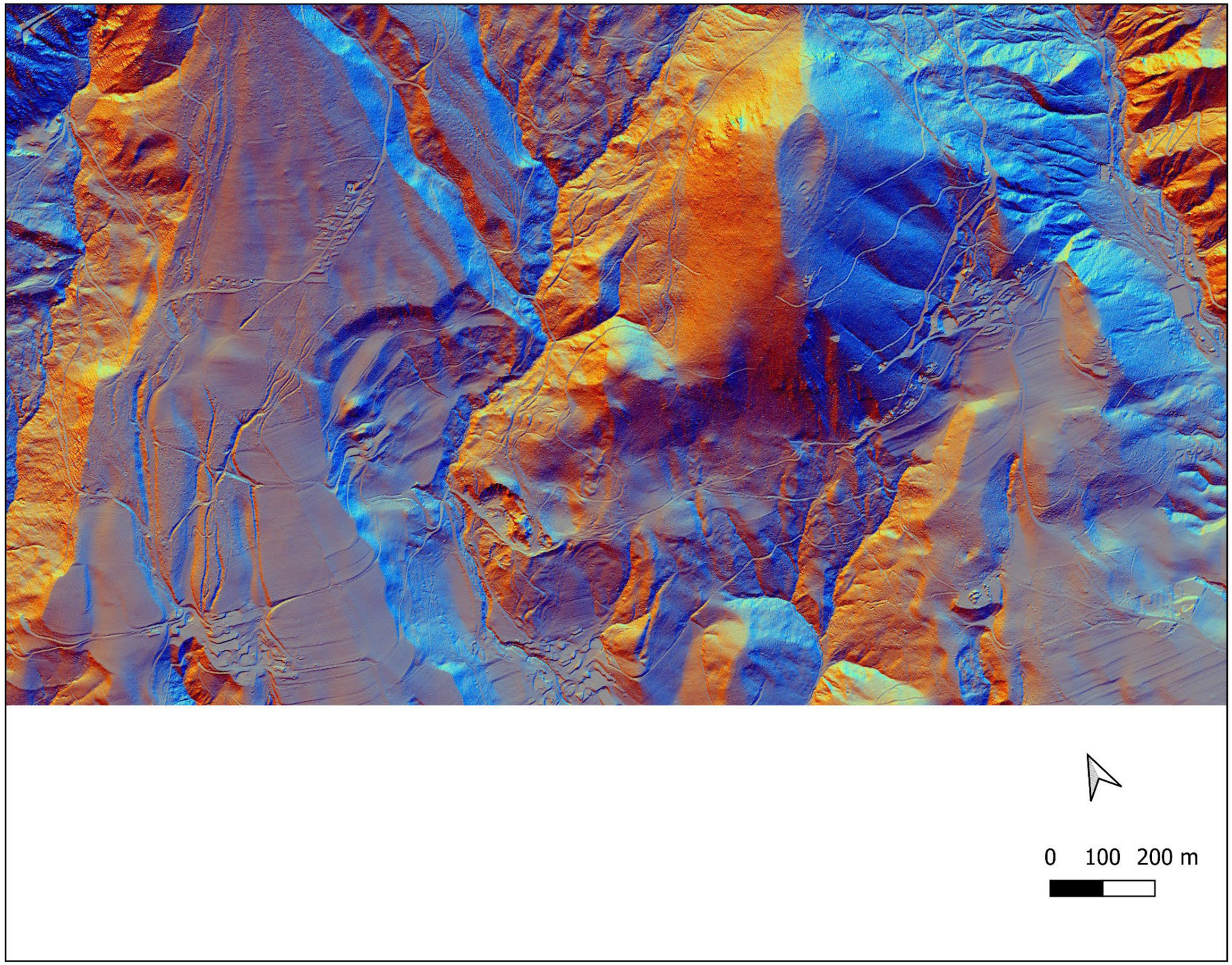

Figure S7: Multidirectional shaded relief from lidar-derived DEM along the Sava Fault in the area of Povlje and Laško.

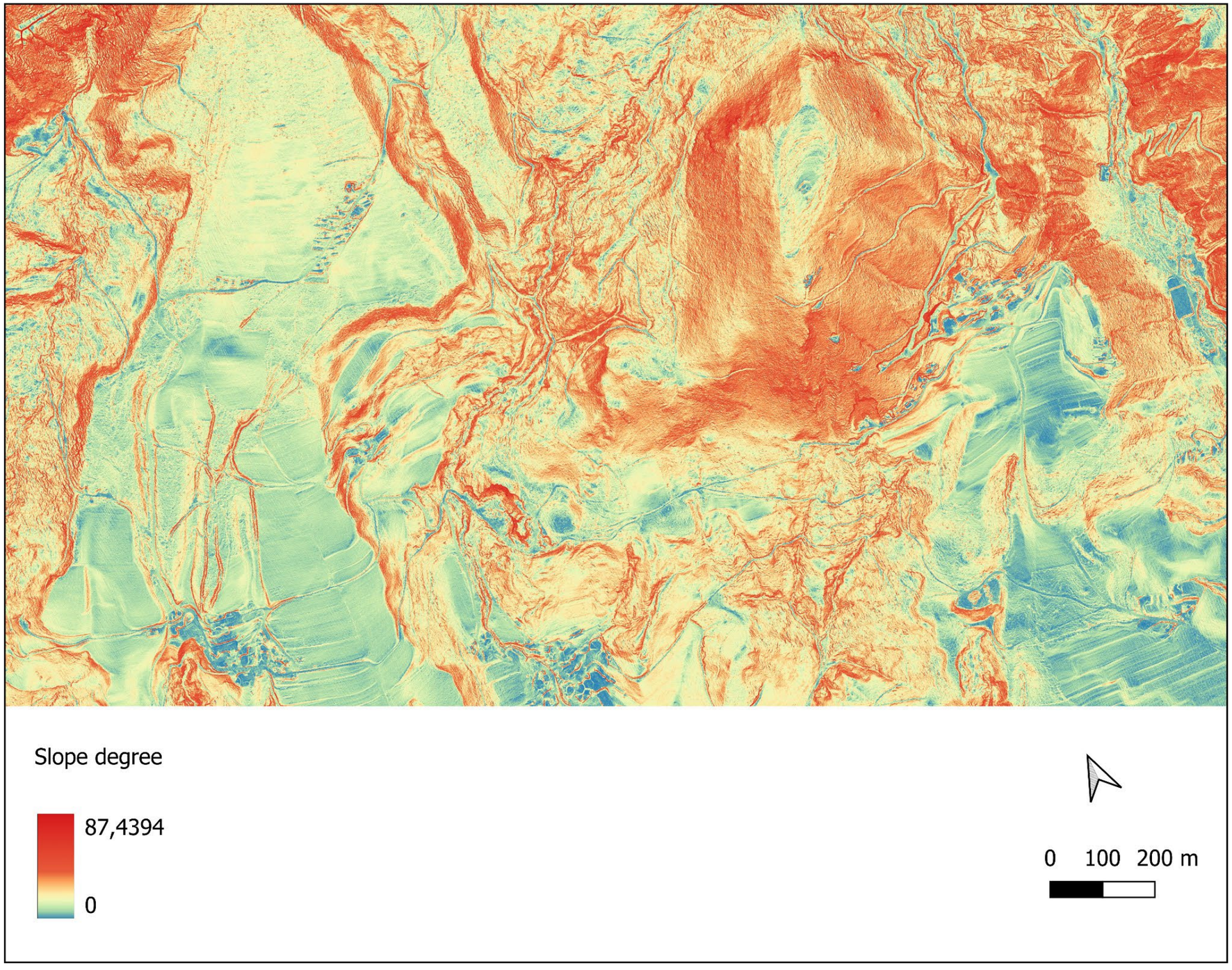

Figure S8: Slope map from lidar-derived DEM along the Sava Fault in the area of Povlje and Laško.

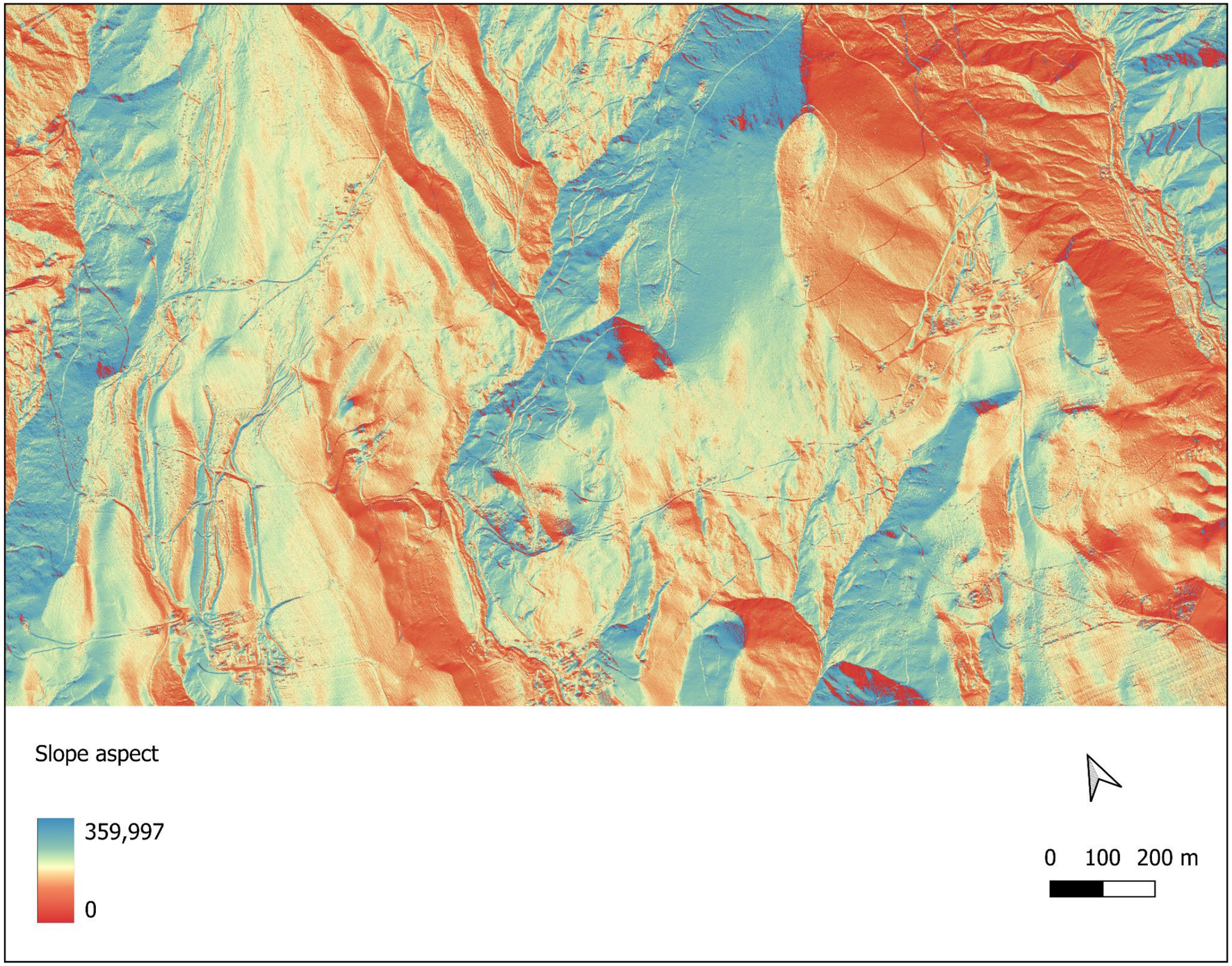

Figure S9: Aspect map from lidar-derived DEM along the Sava Fault in the area of Povlje and Laško.

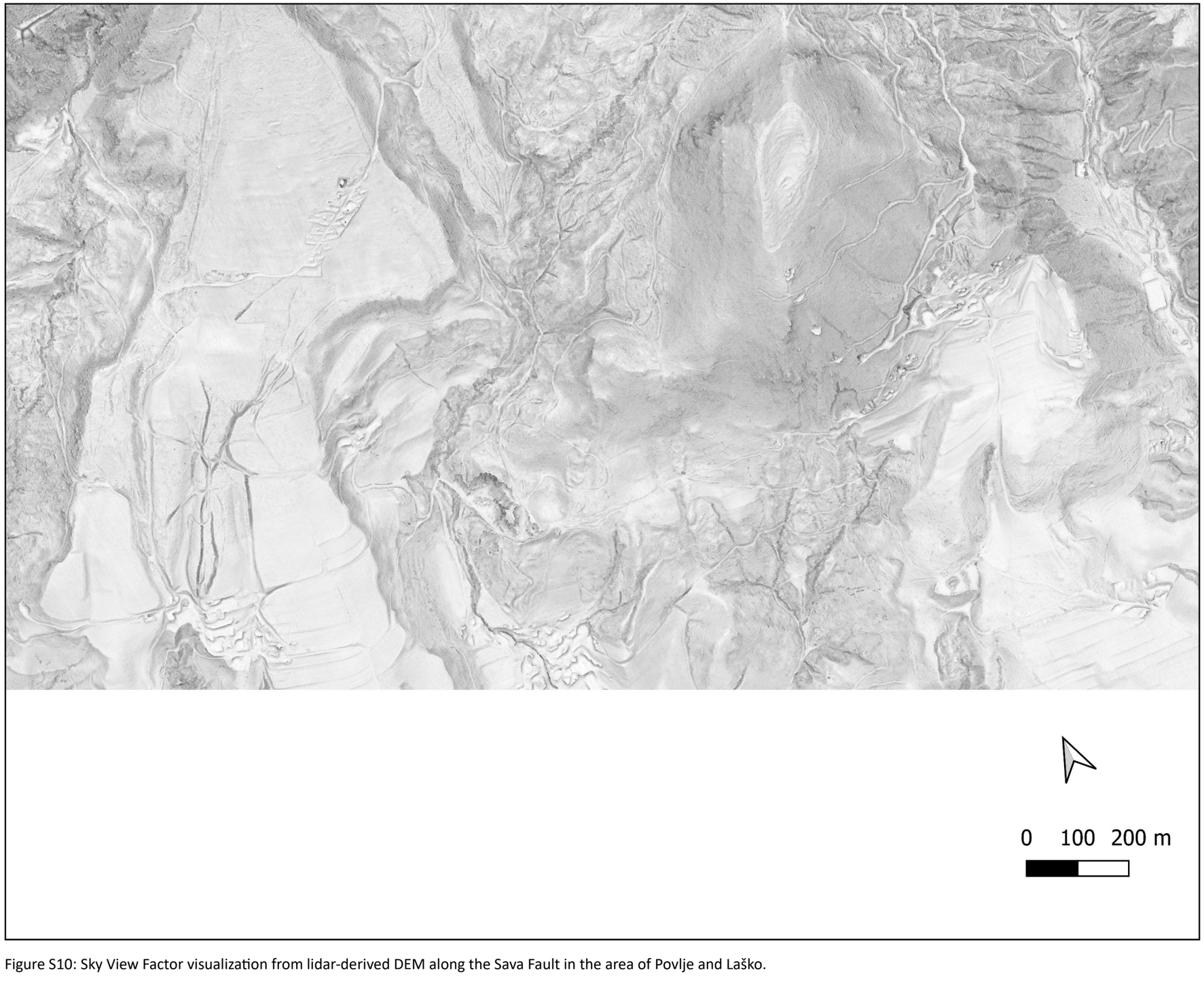

Figure S10: Sky View Factor visualization from lidar-derived DEM along the Sava Fault in the area of Povlje and Laško.

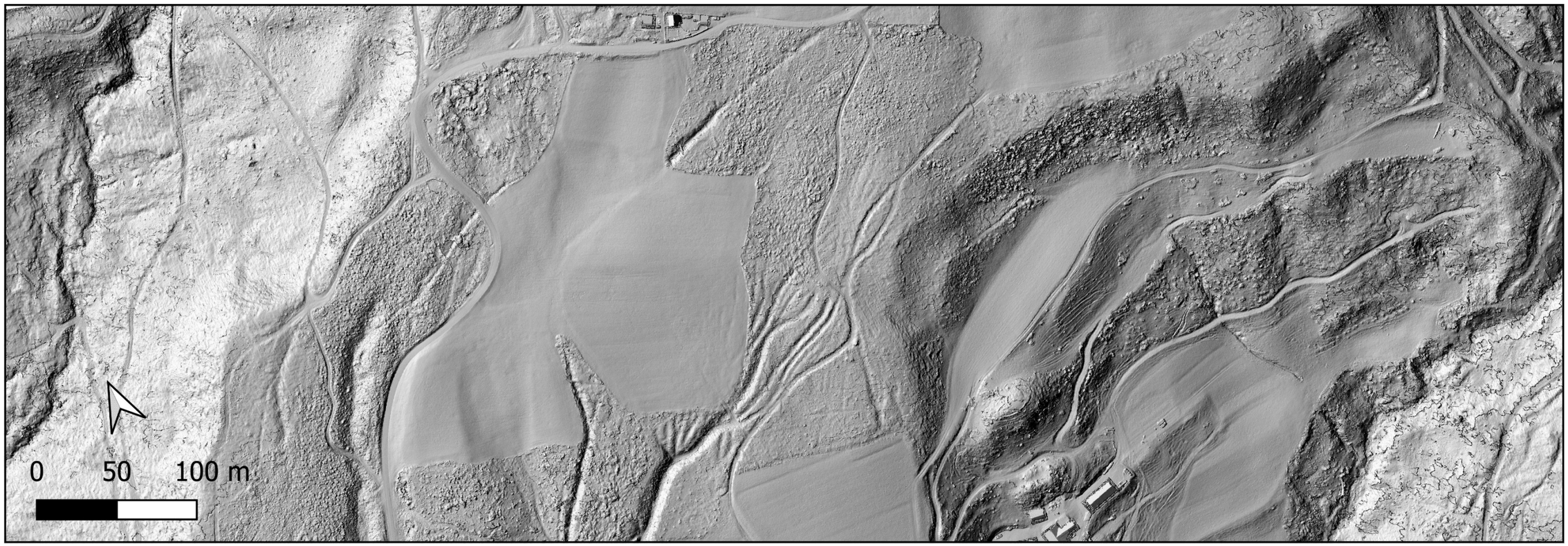

Figure S11: Shaded relief from combined photogrammetric and lidar DEM at Povlje.

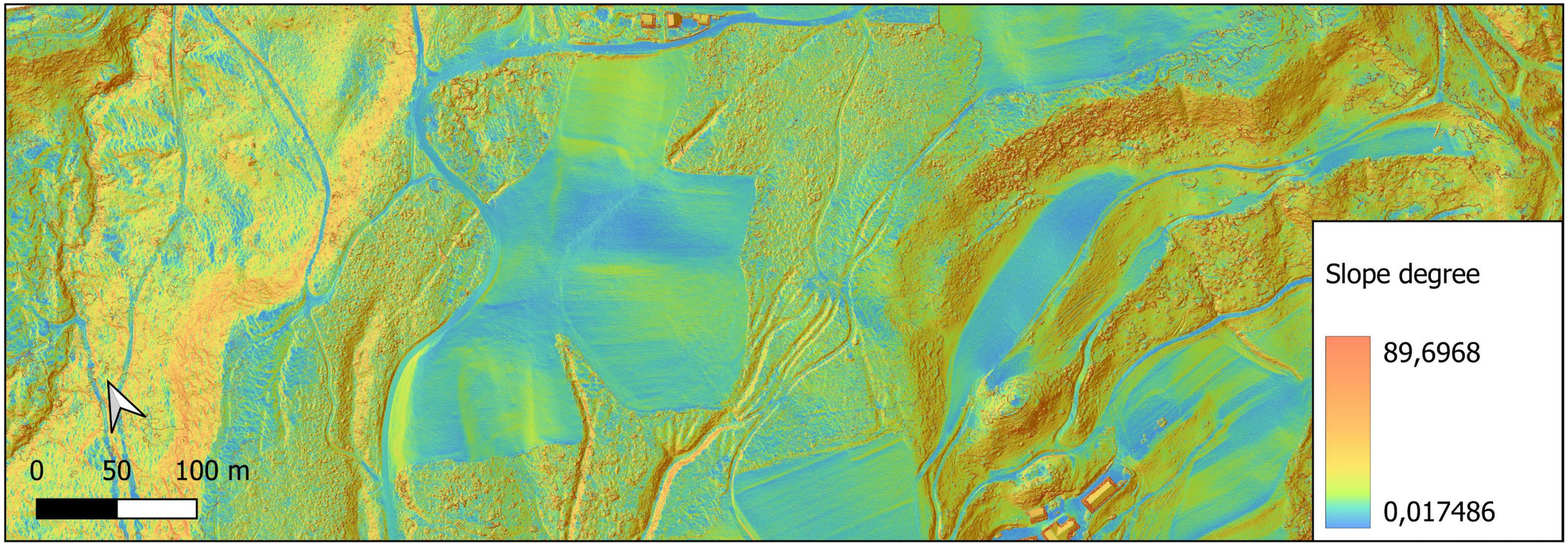

Figure S12: Slope map from combined photogrammetric and lidar DEM at Povlje.

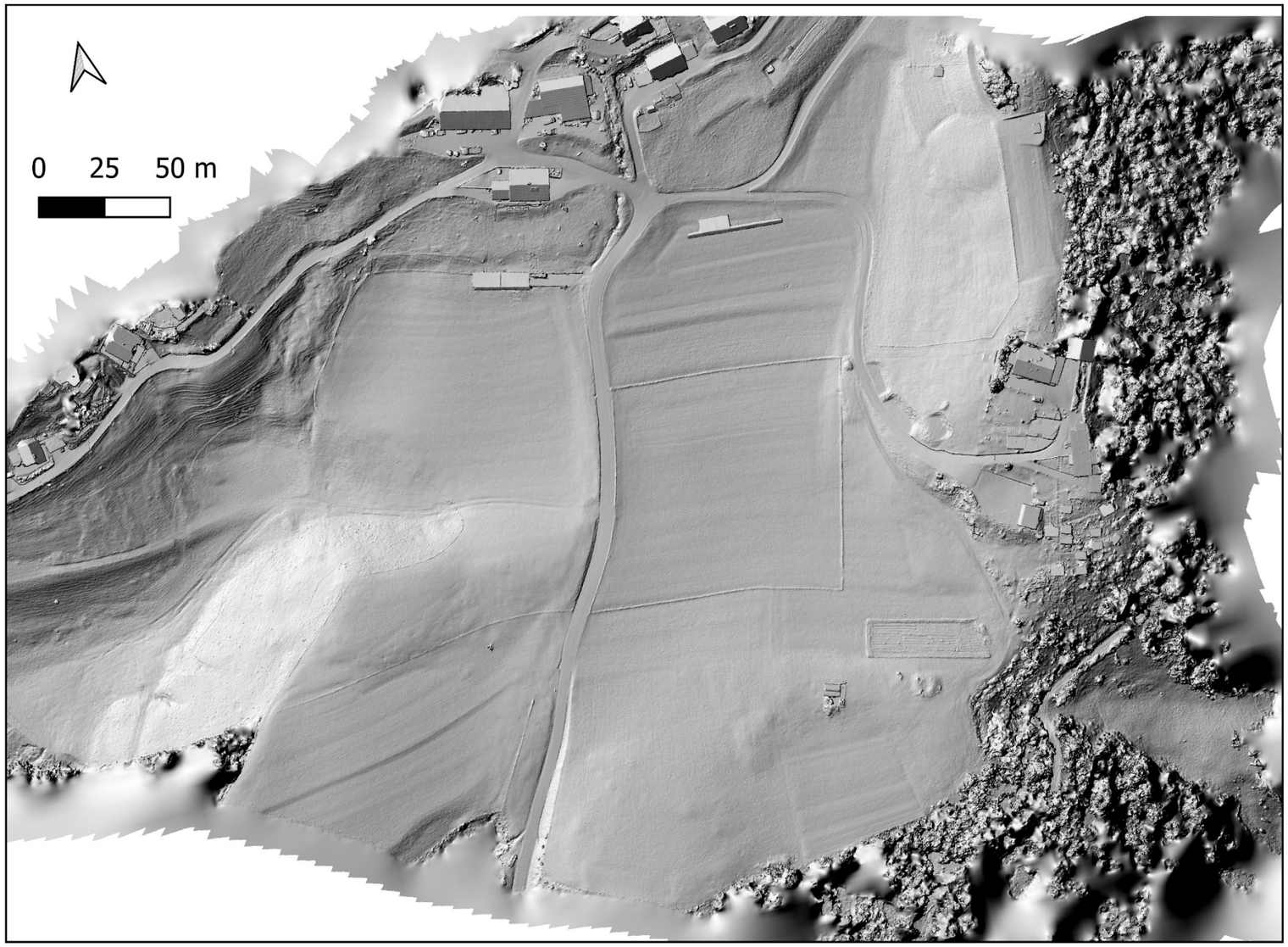

Figure S13: Shaded relief from photogrammetric DEM at Laško.

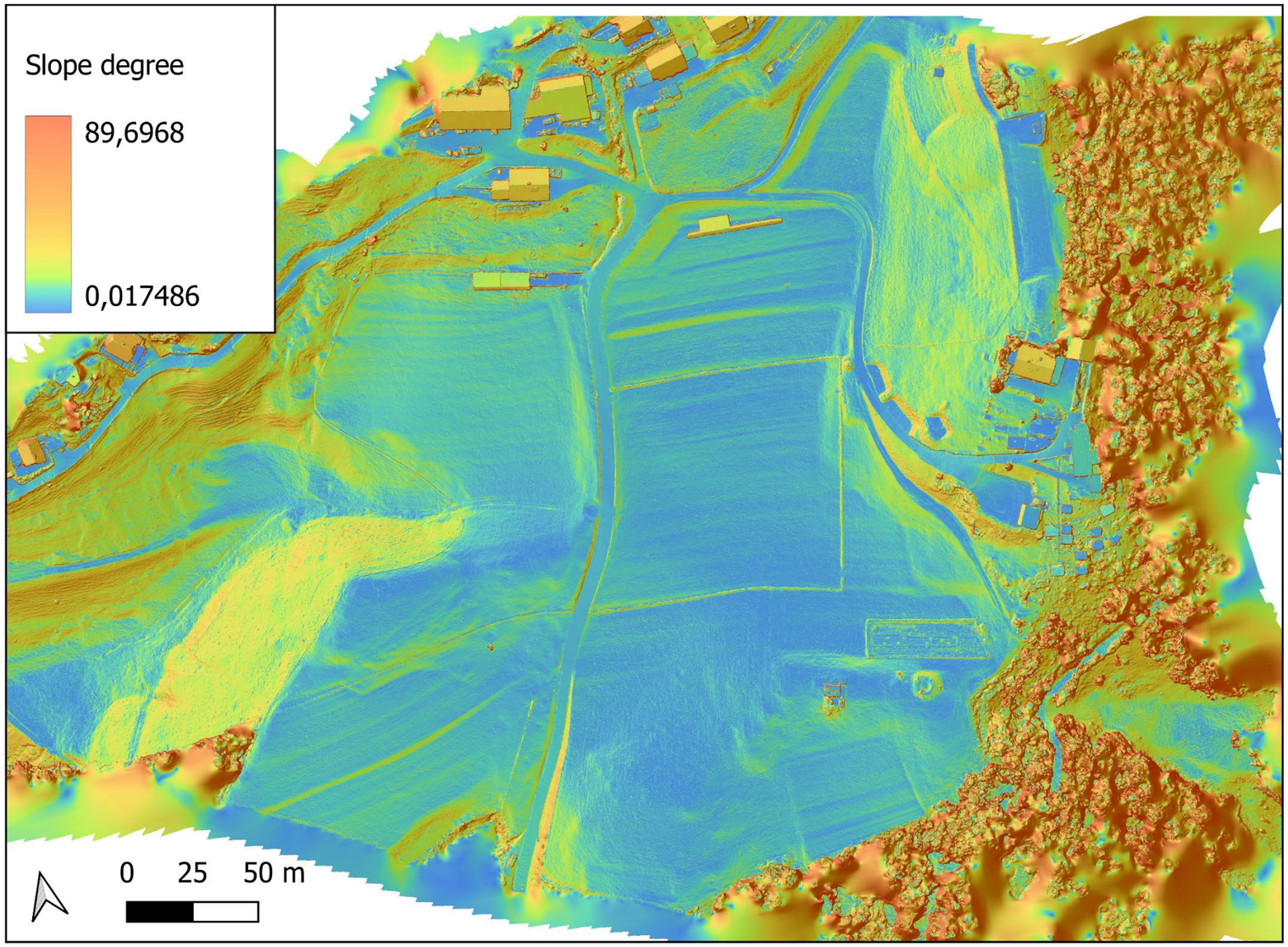

Figure S14: Slope map from photogrammetric DEM at Laško.

Section S2 – Geological map

This section contains the detailed geological map along the Sava Fault between Zalog and Mače near Preddvor (Figure S15), description of litostratigraphic units and structure.

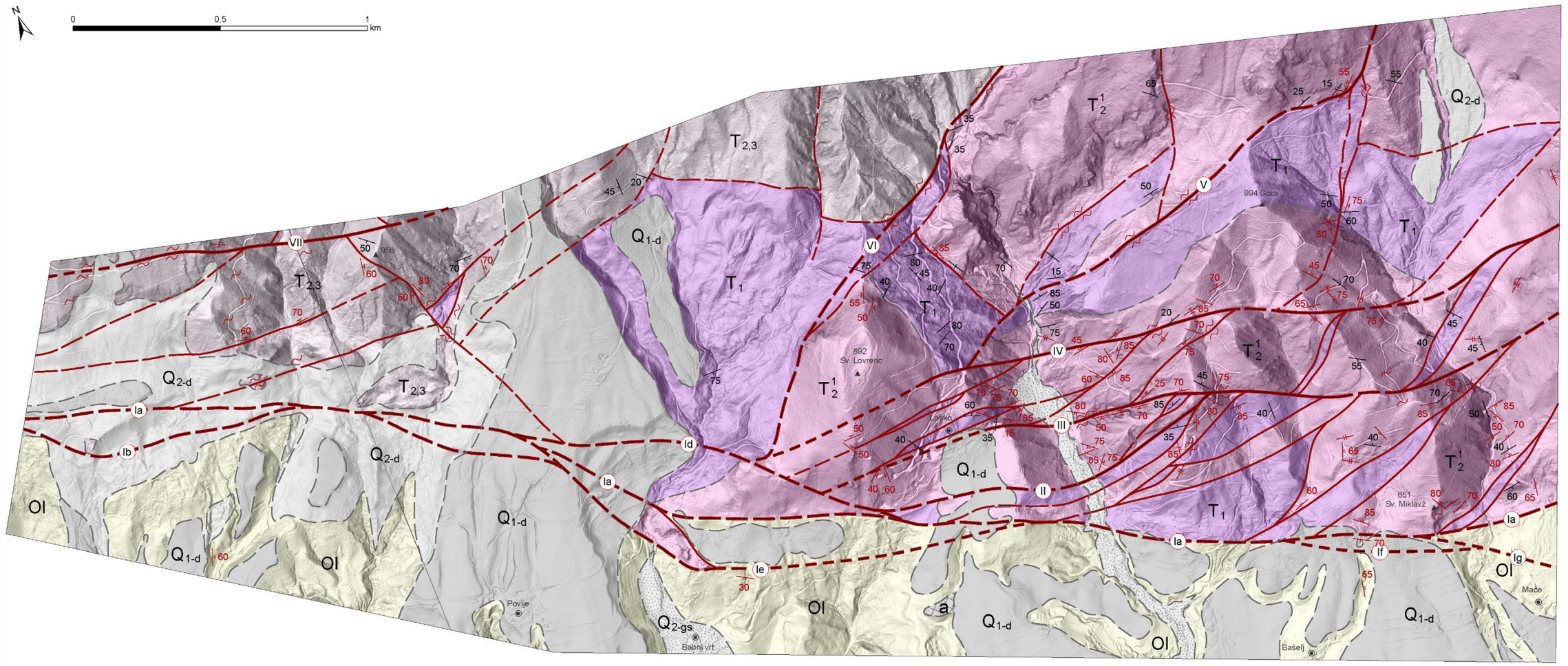

Figure S15: Geological map along the Sava Fault between Zalog and Mače near Preddvor.

Lithostratigraphic Units

Steep hills above Gmajna, Mount St. Lovrenc (918 m), Mount Gore (994 m), and Mount Kozjek (1101 m) north of Povlje, Bašelj, and Mače, as well as the southern slopes of Tolsti Vrh (1715 m), Storžič (2132 m), Mali Grintavec (1813 m), and Srednji Vrh (1853 m), are composed of Triassic rocks. Oligocene rocks form the more gently inclined lower parts of the slopes above Zalog, near Povlje, Babni Vrt, Bašelj, and Mače. Quaternary sediments are deposited on the slopes and in the valleys at the transition from Triassic to Oligocene rocks, effectively covering the fault contact.

Werfen Formation - Lower Triassic (T_1)

The Werfen Formation occurs in a characteristic development that, due to a uniform sedimentary environment in the Early Triassic, is almost the same throughout the Southern Alps and Dinarides [4]. This lithostratigraphic unit is relatively easily recognizable and serves as an excellent marker in structural-geological mapping, distinguishable from otherwise very similar dolomites of different ages.

The lower part of the Werfen Formation typically consists of yellowish-brown layered dolomite, often sandy in appearance and containing muscovite. Above the dolomite, there is yellowish-brown layered marlstone, which transitions into colorful green and purple siltstones and quartz sandstones (Figure S16). The sandstones frequently contain lens-shaped bodies of layered dark gray to dark red calcarenites and ooid limestones. The lower part of the Werfen Formation indicates rhythmic sedimentation.

The upper part of the Werfen Formation typically begins with thick-bedded gray limestone, transitioning into indistinctly layered sandy dolomite. Above that, there is dark gray slaty marlstone, followed by thin layers of occasionally nodular, banded, gray to bluish-gray marly limestone with intercalations of marlstones. The thinly layered and slaty rocks of the Werfen Formation exhibit quickly changing dip angles and smaller folds in many parts of the area under investigation.

The Werfen Formation appears in a highly dissected belt in a general west-to-east direction, north and west of Mount St. Lovrenc above Laško, on the slopes of Mount Gore above Bašelj, and Mount Kozjek above Mače. Contacts with adjacent lithostratigraphic units are predominantly tectonic, with rare occurrences of normal contacts with Anisian Dolomite. The clastic parts of the unit observed in the outcrops are often heavily weathered and prone to erosion processes (Figure S17).

Figure S16: Characteristic development of the clastic Werfen Formation with purple sandstones, gray siltstone and marlstone and dark gray marly limestones.

Figure S17: Strongly cleaved rocks of the Werfen Formation in a tectonic lens in a quarry north of Povlje.

Anisian Beds - lower part of Middle Triassic (T_2^1)

The Anisian Beds lie with a normal geological boundary on the Werfen Formation (Figure S18). They are predominantly represented by dolomite, with occasional occurrences of limestone in between. The Anisian Dolomite is dark gray and layered in the lower part. In certain layers, there is stromatolitic lamination, which is helpful in determining stratification in tectonized cleaved zones (Figure S19).

Upward, the dolomite quickly becomes lighter gray and indistinctly layered to massive, with intercalated layers of light gray limestone, dolomitized limestone, and dolomitic breccia. Generally, the Anisian dolomite is heavily fractured or shattered. The Anisian Dolomite forms the majority of the investigated area, covering the entire northeastern part between Gradišče and Kisovec, as well as further south between Krničar, Laško, Suh Vrh, and Studenci.

Figure S18: A ravine developed along a stratigraphic contact between the thin-bedded clastic rocks of the Werfen Formation and the Anisian Dolomite.

Figure S19: Anisian Dolomite in a shattered fault zone displaying indistinct stratification and densely spaced fracture cleavage.

Schlern Formation - Middle and Upper Triassic (Upper Ladinian-Lower Carnian) ($T_{2,3}$)

The Schlern Formation is in tectonic contact with older Triassic units in the northern part of the mapped area. In the northwestern part of the area, north of Povlje and Zalog, it is in tectonic contact

with Oligocene mudstones and marlstones in the south. The contact is covered by extensive slope debris from the Schlern Dolomite in the hinterland.

The Schlern Formation is represented by white and light gray massive dolomite, occasionally exhibiting indistinct layering. It is often sparitic (coarse-grained) and porous. It is frequently difficult to distinguish it from the Anisian Dolomite, especially when they are in tectonic contact. This dolomite is also heavily fractured or shattered throughout most of the area (Figure S20). Tectonic zones several meters wide in the cross-section of outcrops are common.

In fault zones, brecciated cataclastic texture with yellowish and reddish matrix is often present, and there are fractured zones with fracture systems in multiple directions that continue into heavily shattered (crushed) structureless zones (Figure S21). The Schlern Dolomite forms the northwestern part of the investigated area from Gradišče to the southern slope of Storžič.

Figure S20: Tectonized, light gray to white, massive Schlern Dolomite.

Figure S21: Tectonic zones in the Schlern Dolomite: cohesive and incohesive fractured portions alternate within the outcrop north of Povlje.

Alternation of marlstones and mudstones - Oligocene (Ol)

Oligocene marlstones and mudstones represent rocks formed in a marine sedimentary environment. Their distribution in the investigated area is limited to the north with a fault where they are in tectonic contact with Anisian Beds and the Werfen Formation, and to the northwest with rocks of the Schlern Formation. Oligocene marlstones and mudstones are heavily fractured and cleaved, indicating significant tectonic deformation. They are characterized by their non-layered nature.

The marlstones and mudstones are gray in color and are mostly exposed along stream channels (Figure S22). They occur from the southwest to the southeast part of the map. They are mostly covered by Pleistocene diamicts, particularly in the vicinity of Povlje, Laško, and Bašelj. To a lesser extent, in the area of Babni Vrt and Bašelj, they are overlain by Holocene gravel and sand, and in the area of Stari Dvor and Gmajna, also by Holocene diamict.

Figure S22: Cleaved Oligocene mudstones in the bed of a small unnamed stream between Zalog and Povlje.

Andesitic tuff - Oligocene (Ol)

The tuff occurs in normal and tectonic contact with Oligocene marlstones and mudstones. It is green in color and often weathered due to oxidation, giving it a characteristic reddish-brown color. It contains black and white weathered inclusions (lapilli), which are presumed to belong to mafic minerals and plagioclase. The tuff is present in a smaller area on the western part of the map, along the Sevnica stream and west of it, as well as in a fault zone east of Bašelj.

Diamict - Pleistocene (Q_1-d)

Pleistocene diamicts are deposited over tectonic contacts between Triassic and Oligocene rocks and overlying Oligocene rocks. They occur at higher elevations above present-day valleys and ravines. Geomorphologically, they represent fans or remnants of terraces.

The largest fan is located near Povlje and consists of diamict with angular to subangular clasts, including blocks up to 1 meter or more in size, with a fine-grained sandy to muddy matrix (Figure S23). The material transport was relatively short, considering the hinterland, and the fan itself is steep. Based on the composition and morphology of the fan, it is inferred that these sediments are from debris flows. The thickness of the fan is estimated to be up to 20 meters.

West of the Povlje fan, the diamict is found in erosional remnants above the Oligocene rocks. The planar surface at Laško consists of diamict with block sizes reaching several meters (Figure S24). We did not find any outcrops allowing a detailed examination of the sediment at Laško. Considering the block sizes and the geomorphological position of the planar surface at the transition from the mountains to the Pleistocene depositional level, it is likely that these are debris flow sediments.

Further toward the southeast, diamicts occur in erosional remnants of fans deposited over Oligocene rocks south of the tectonic contact with Triassic rocks. In one of these remnants, east of Bašelj, we found an outcrop of several meters thick diamict with subrounded limestone and dolomite clasts up to 40 cm in size, within a sandy-silty matrix (Figure S25). At higher elevations northeast of Povlje, the unit occurs as diamictite – cemented slope debris (Figure S26).

Figure S23: Diamict of Povlje alluvial fan.

Figure S24: Large blocks of carbonates lying on the Laško surface are part of the diamict deposited over the clastic rocks visible in the base.

Figure S25: Pleistocene diamict outcrop east of Bašelj.

Figure S26: Pleistocene diamict NE of Povlje. It consists mostly of carbonate clasts.

Gravel and sand - Holocene (Q_2-pp)

Gravel and sand occur in narrow valleys of streams crossing the Sava Fault. These are fluvial sediments deposited in Holocene floodplains. Due to the prevailing carbonate hinterland, fluvial sediments in the area are mainly represented by gravel and sand, whereas in areas where they are deposited over Oligocene rocks, silt and clay are also present.

Diamict - Holocene (Q_2-d)

Holocene diamict covers slopes and occurs primarily in the area of tectonic contact between the Schlern Formation and Oligocene marlstones and mudstones in the western part of the map. It mostly lacks preserved sedimentary landforms; we infer that it is genetically a colluvium, slope debris, and/or debris flow sediment, or a mixture of these.

In the upper part of the slope in the far western part of the map, the diamict is mostly slope debris, which can be more than 10 meters thick. Angular and subangular clasts predominate within a sandy matrix (Figure S27). It is poorly sorted; the largest blocks can be larger than 1 m^3. The clasts consist of the rocks of the Schlern Formation, which form the tectonized walls in the hinterland.

Holocene diamict also occurs in the form of a slope debris fan, deposited in a ravine on the steep slopes of Suha in the northeastern part of the map.

Figure S27: Thick slope debris in the lower part of the slopes north of Zalog.

Anthropogenic landfill - recent (a)

Anthropogenic landfill is located on Oligocene marlstones and mudstones, at the contact with the Pleistocene diamict. This is a small landfill of mineral resources between Bašelj and Babni Vrt.

Structure

The Sava Fault Zone, characterized by a northwest-southeast orientation, separates Triassic rocks from Oligocene rocks in the study area. The fault zone is denoted as "I" on the geological map (Figure S1), with sub-branches labeled from "Ia" to "Ig" representing individual fault sections. Although the fault itself is covered, its intersection with the topography suggests a steep northward dip. East of Povlje, the fault bends, indicating a releasing right bend between Povlje and Laško (Id, Ia, and Ie branches). Moving eastward, multiple secondary faults diverge in a west-southwest direction (II, III, IV), exhibiting steep to subvertical dips toward the south (III, IV) or north (II). Interspersed among these faults are several minor parallel faults running in a south-west-northeast direction, occasionally demarcating slices of the Werfen Formation and Anisian Beds. Further north, there are less steep faults dipping to the south (V, VI) and unnamed minor parallel faults branching off from fault IV, trending south-west-northeast. These faults uplift the Werfen rocks above the Anisian Beds. Left-lateral faults in a south-north to southwest-northeast direction additionally disrupt the Anisian rocks. The eastern boundary of the Schlern Formation is marked by a steep fault (VI), separating it from the Anisian Beds and Werfen Formation.

North of Povlje, a tectonic slice of Werfen Formation rocks in contact with the Schlern Formation was delineated (Figure S28). West of Povlje, the tectonic contact between Oligocene rocks and the Schlern Formation is represented by two branches of the main fault labeled Ia and Ib. Adjacent to the main fault zone, a more prominent subvertical fault (VII) was observed, striking northwest-southeast and traversing the Schlern Formation along its entirety on the map. Multiple weaker faults connect

fault VII and Ia, extending in a west-southwest to east-northeast direction. A northwest-southeast trending fault was mapped north of Povlje, serving as a connecting fault between approximately parallel stronger faults. West of this fault, the Oligocene rocks are directly juxtaposed with the Schlern Formation through faults Ia and Ib, while to the east, the Oligocene rocks are in contact with either the Anisian Dolomite or the Werfen Formation.

At the fault contacts between thinly layered Werfen clastic rocks and thick-bedded to massive Anisian dolomites and limestones, the Werfen rocks display small fault-related folds (Figure S29) and are sometimes entrained within tectonic lenses in disrupted layers of Anisian Dolomites (Figure S30). Both formations exhibit significant tectonic deformation at the fault contacts (Figures S31-S32).

Figure S28: Tectonic lens of the Werfen clastic rocks (lower part of the slope, gray-yellow color) in contact with dolomite of the Schlern Formation (upper part of the slope, light gray color) along the non-marked minor fault north of Povlje, between fault VII and Ia.

Figure S29: Thin beds of violet-red and gray Werfen sandstones, claystones, and marlstones, which are folded into a small recumbent fold just below the fault boundary with the Anisian Beds. This photo is taken along the non-marked fault in the gully on the NE foot of Gora (994).

Figure S30: Small tectonic lenses of gray Werfen marlstones intruded between fractured Anisian Dolomite along the minor non-marked fault - the one that runs almost parallel to the NW of fault V.

Figure S31: Tectonic boundary between Anisian Dolomite and Werfen clastic rocks along the V fault.

Figure S32: Anisian Dolomite in an intensely fractured tectonic zone of V fault with differently oriented fault planes. Slickensides are visible on some planes.

Section S3 – Electrical Resistivity Tomography profiles

This section contains uninterpreted versions of the ERT profiles presented in the paper (Figure S33) and additionally version with homogenous color scale for both Laško and Povlje profiles (Figure S34).

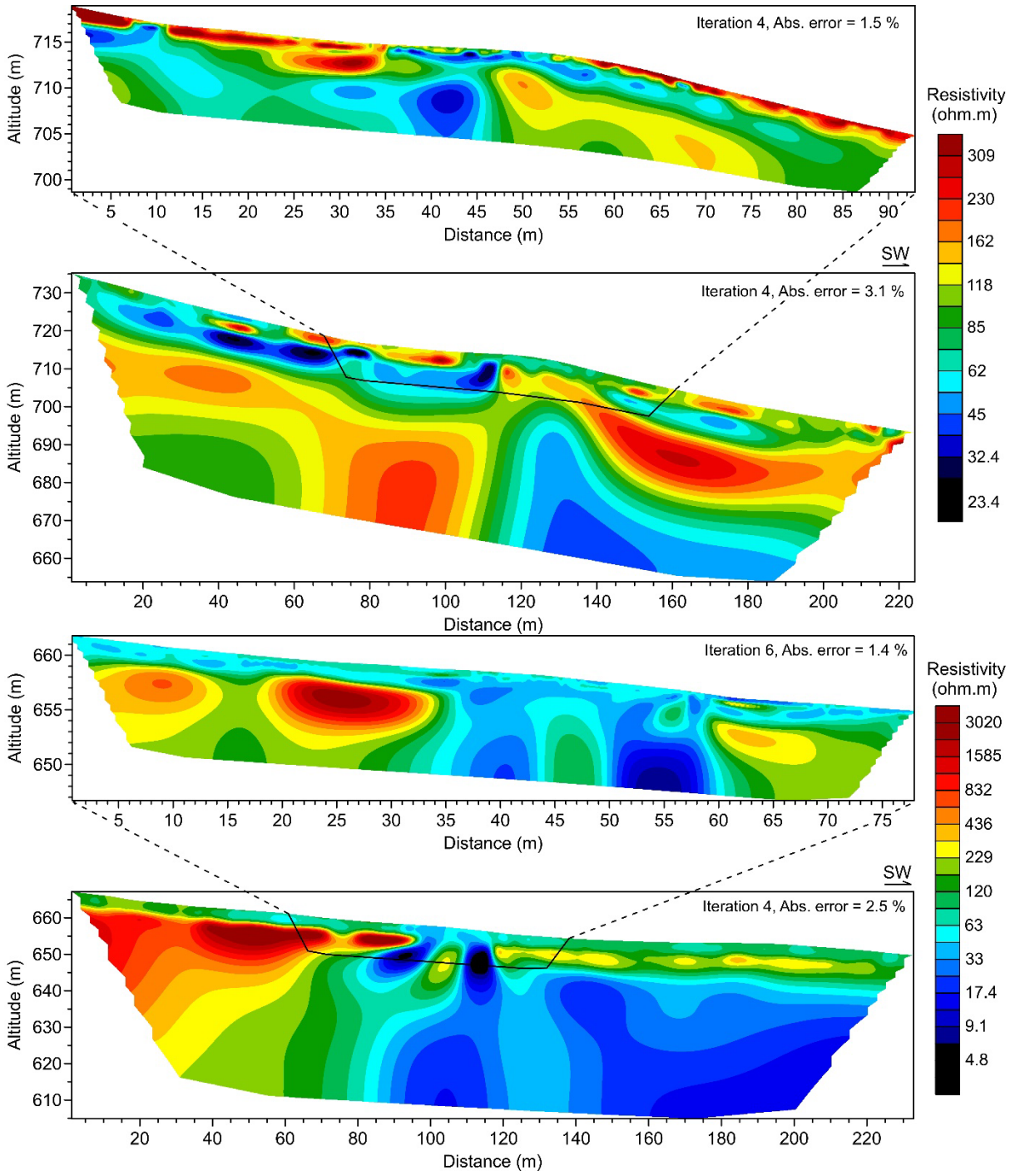

Figure S33: ERT profiles across the Sava Fault at the locations Povlje and Laško. From top to bottom: Povlje 2, Povlje 1, Laško 2, Laško 1.

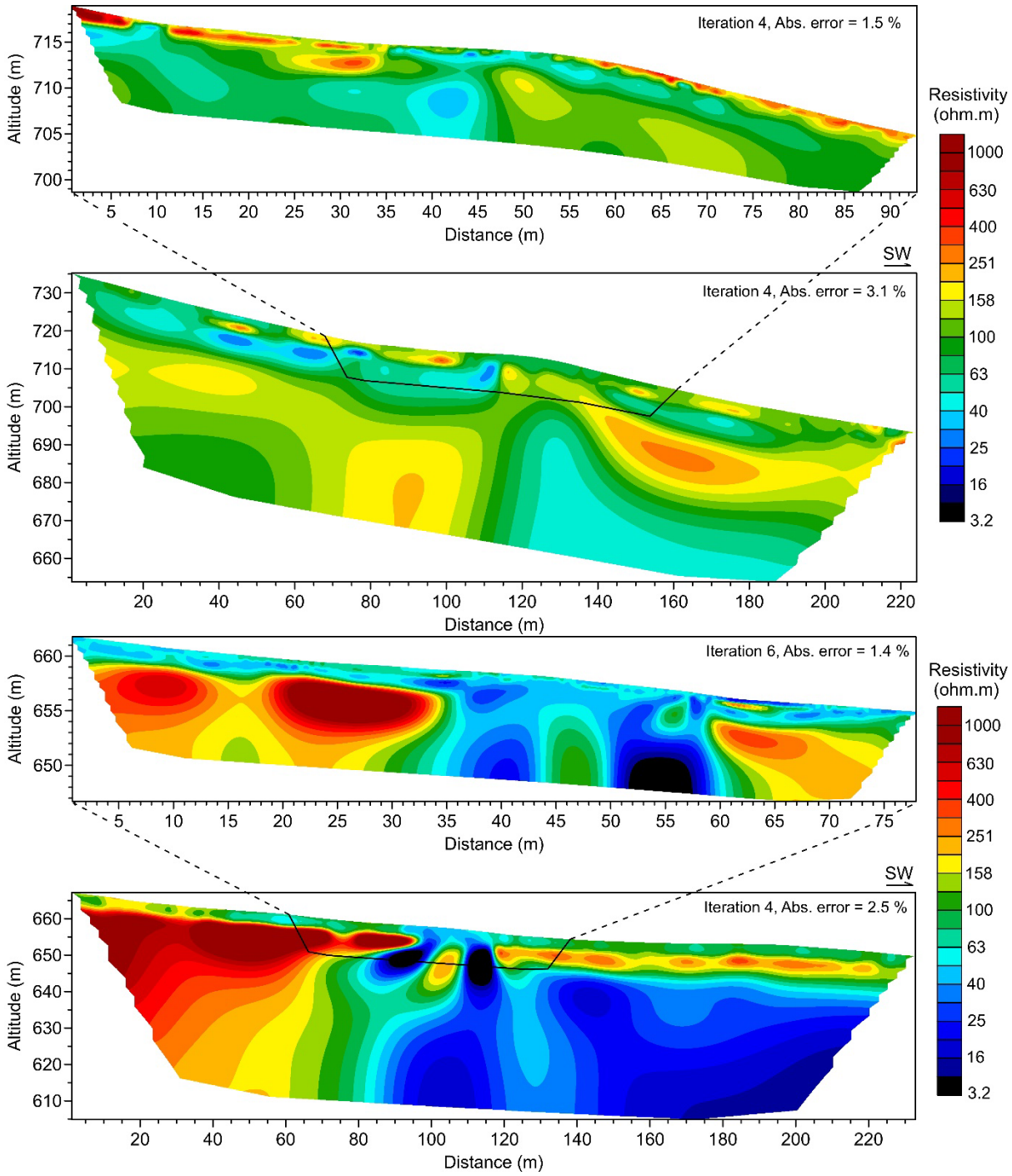

Figure S34: ERT profiles across the Sava Fault at locations Povlje and Laško; homogenous color scale. From top to bottom: Povlje 2, Povlje 1, Laško 2, Laško 1.

Section S4 – Ground Penetrating Radar profiles

Here we present the uninterpreted and interpreted versions of all GPR profiles (Figures S35-S42) and their comparison with ERT profiles (Figures S37, S38).

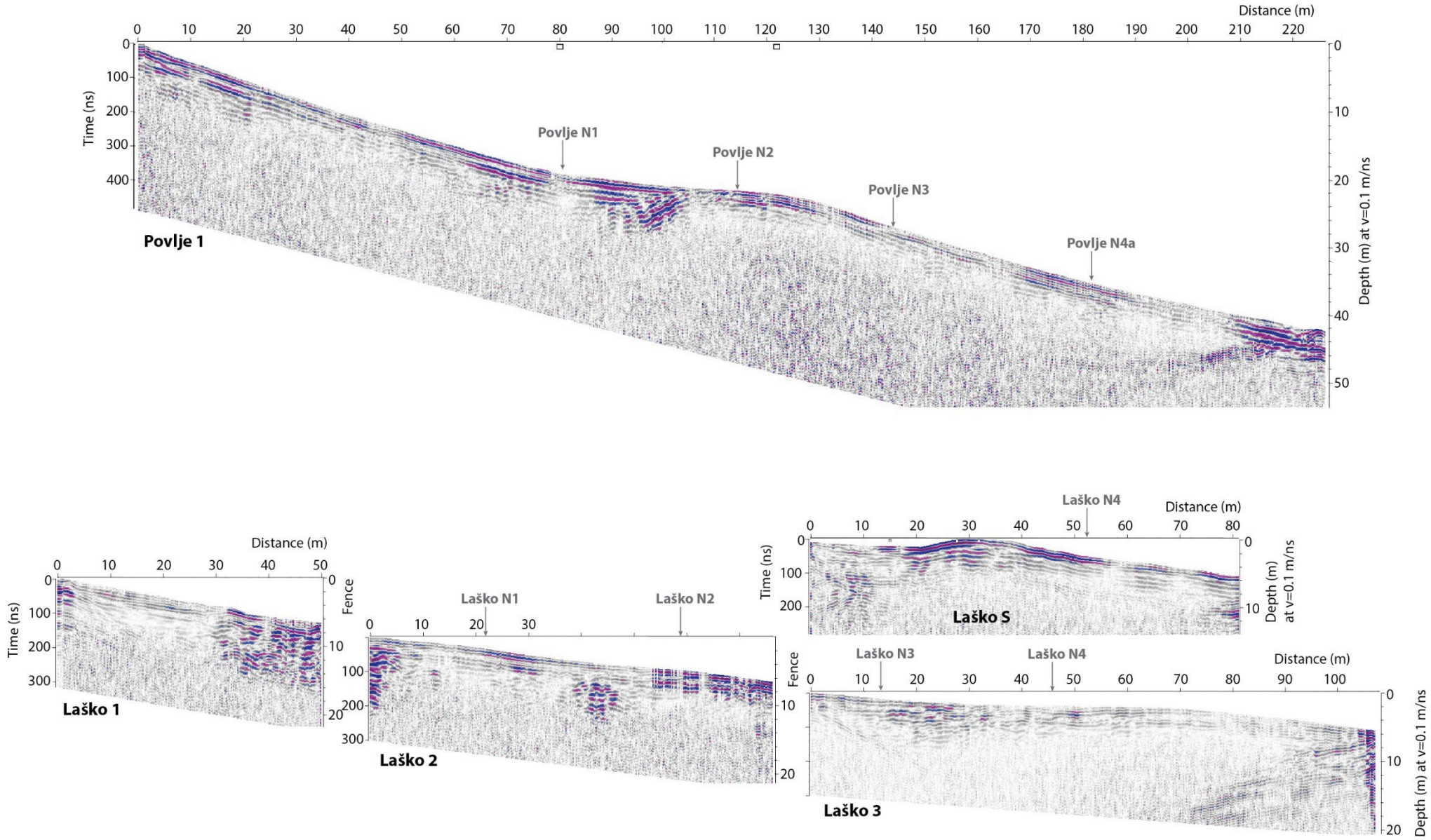

Figure S35: GPR profiles across the Sava Fault at locations Povlje and Laško.

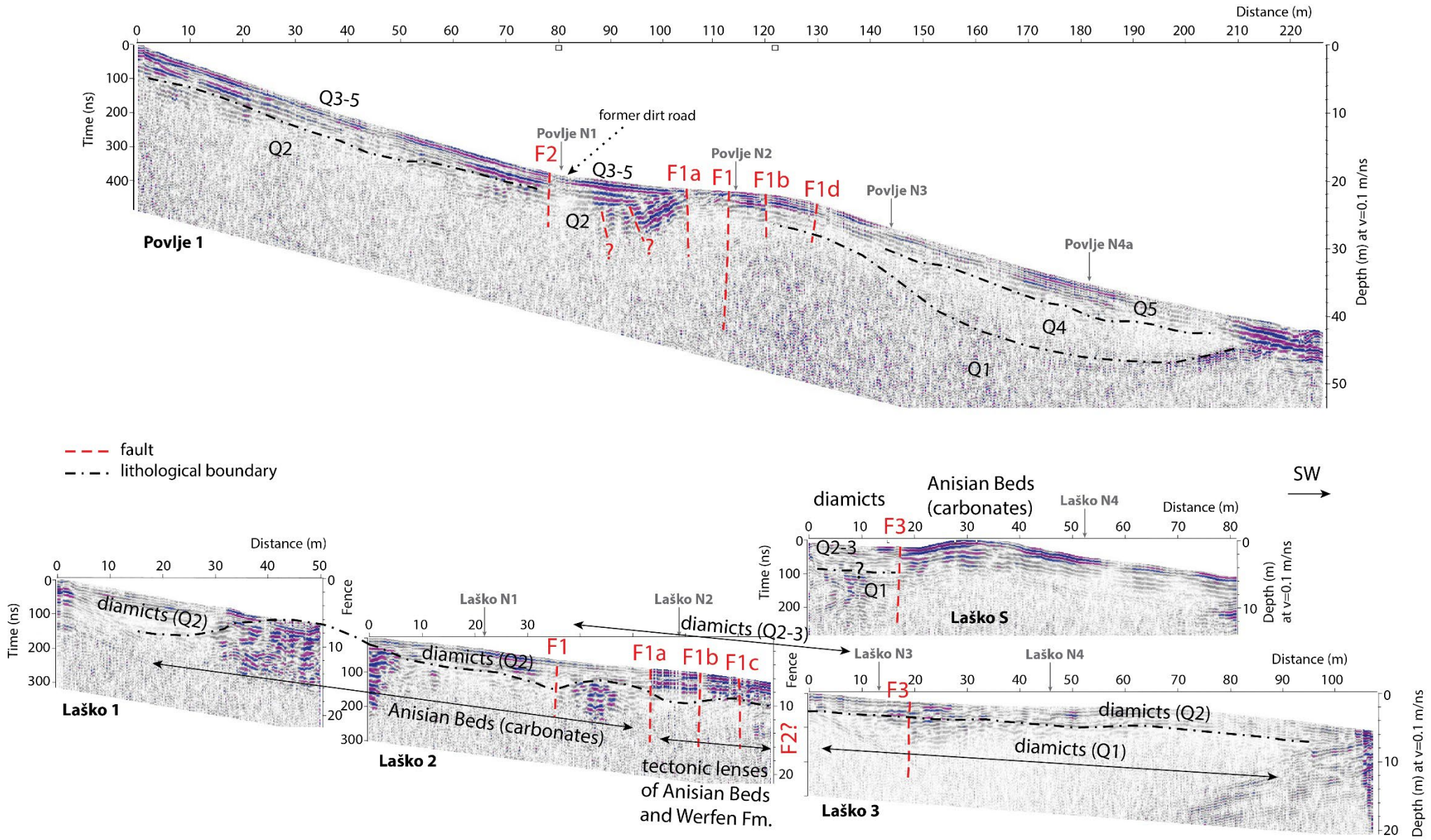

Figure S36: GPR profiles across the Sava Fault at locations Povlje and Laško. The GPR lines match with the ERT lines - see Figures 5 and 6 in the paper for location of the profiles. Interpretation is based on radargram characteristics and results of ERT survey, tectonic geomorphological and structural-geological field mapping.

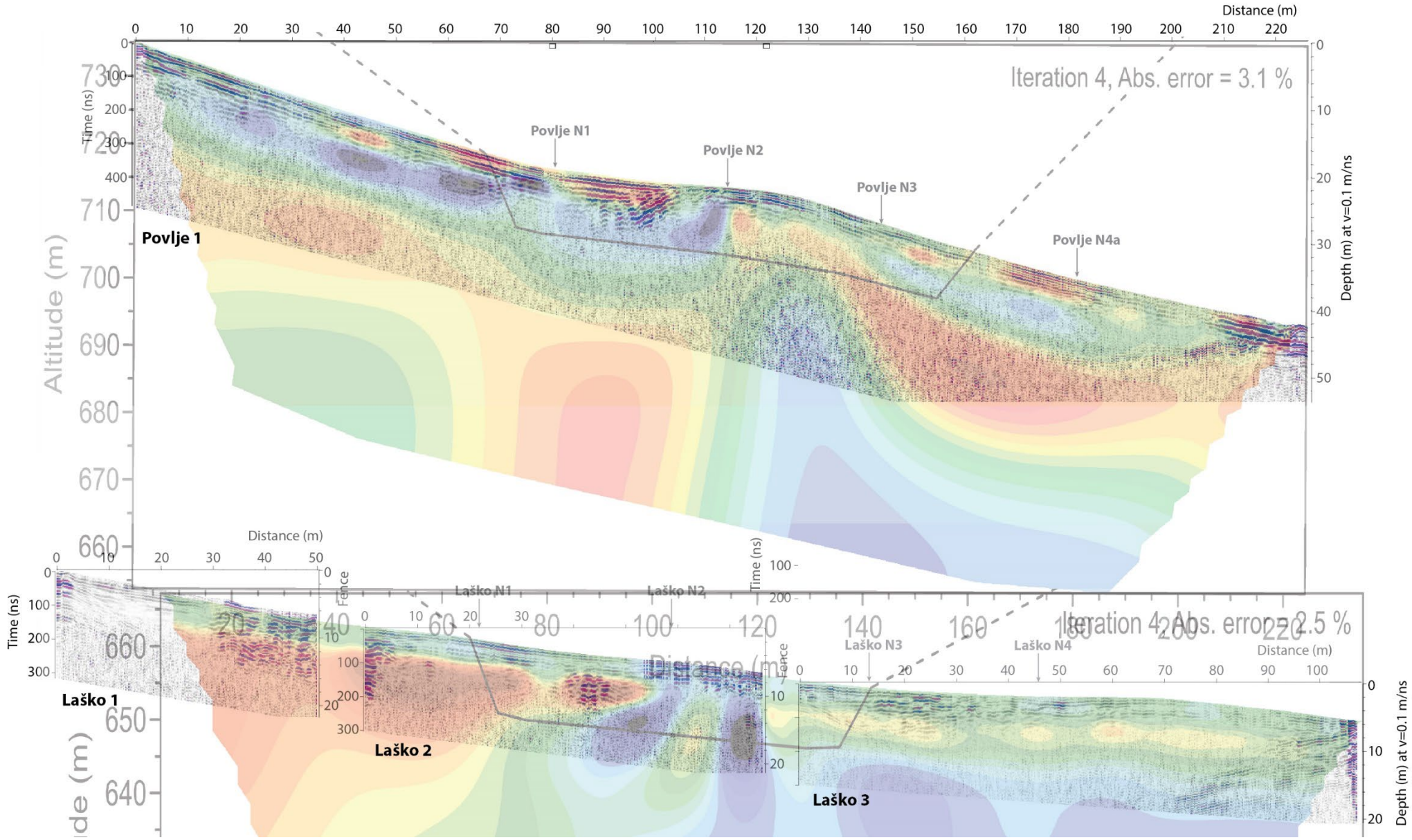

Figure S37: GPR profiles across the Sava Fault at locations Povlje and Laško overlain by ERT profiles with 5 m electrode spacing. For resistivity values see Figure 8 in the paper.

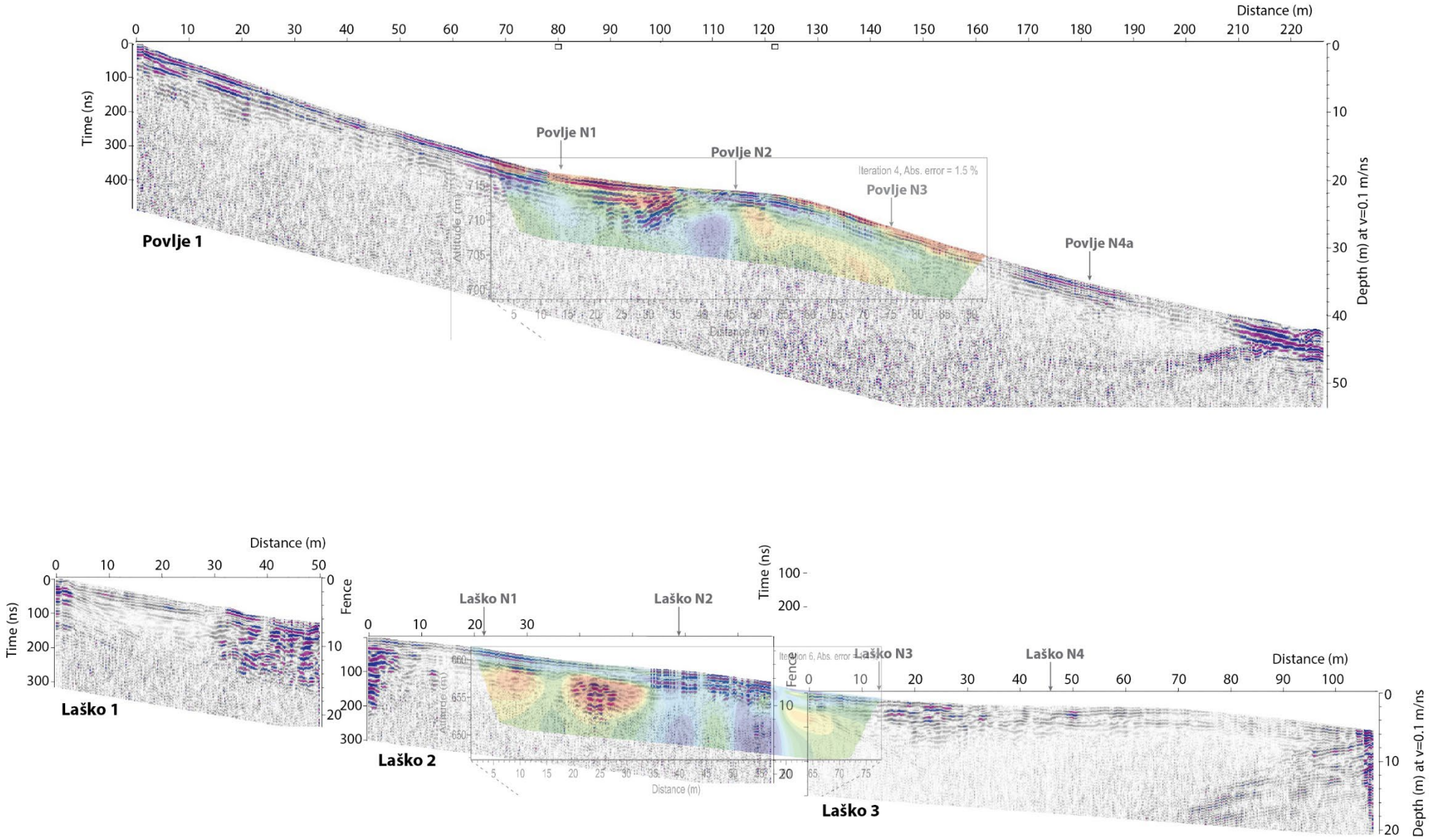

Figure S38: GPR profiles across the Sava Fault at locations Povlje and Laško overlain by ERT profiles with 1 m electrode spacing. For resistivity values see Figure 8 in the paper.

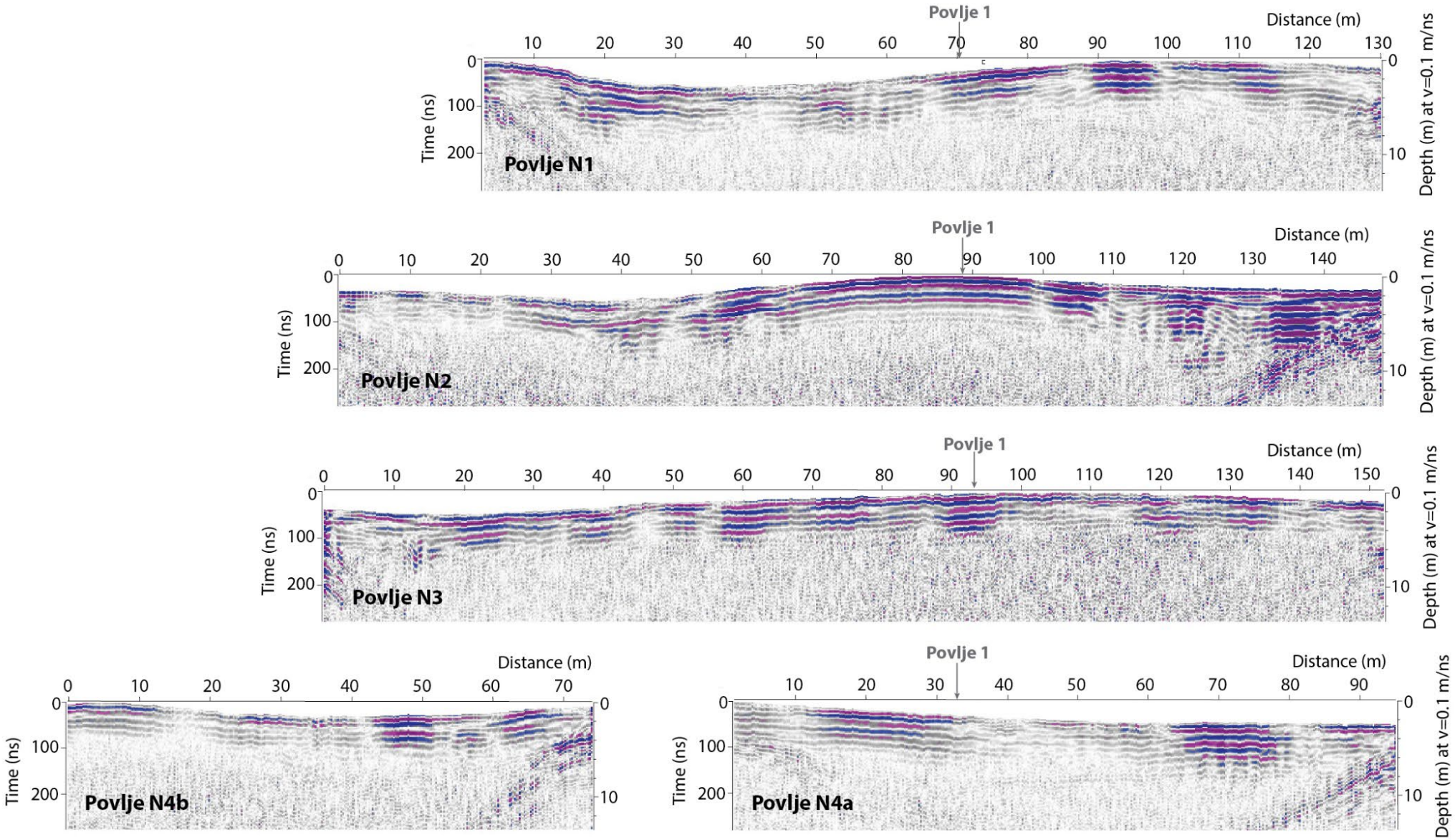

Figure S39: GPR profiles parallel to the Sava Fault at location Povlje.

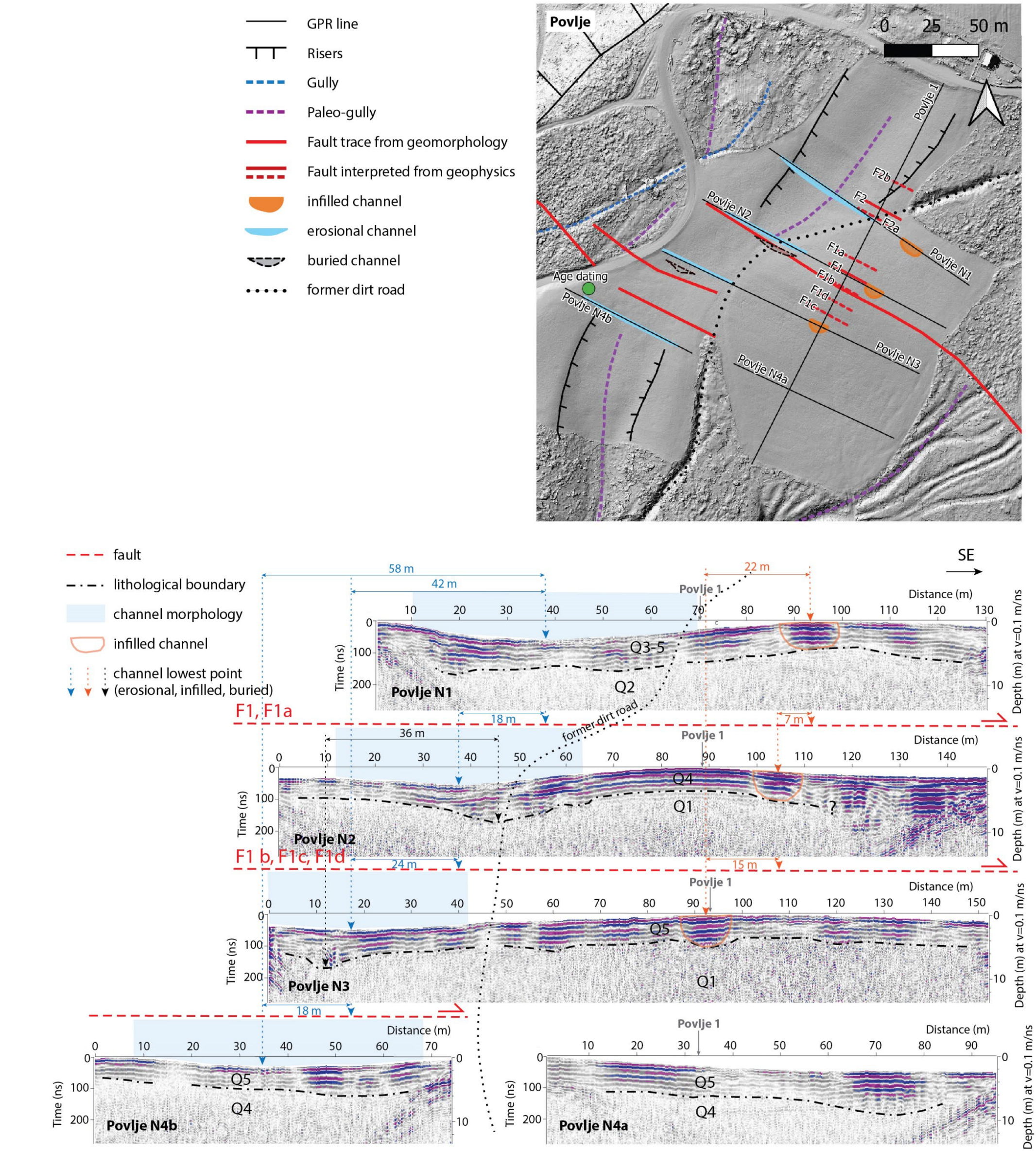

Figure S40: GPR profiles parallel to the Sava Fault at location Povlje. Interpretation is based on radargram characteristics, comparison with fault perpendicular GPR and ERT profiles, tectonic geomorphological and structural-geological field mapping. See the paper for explanation of the measured displacements (blue, orange, and black arrows).

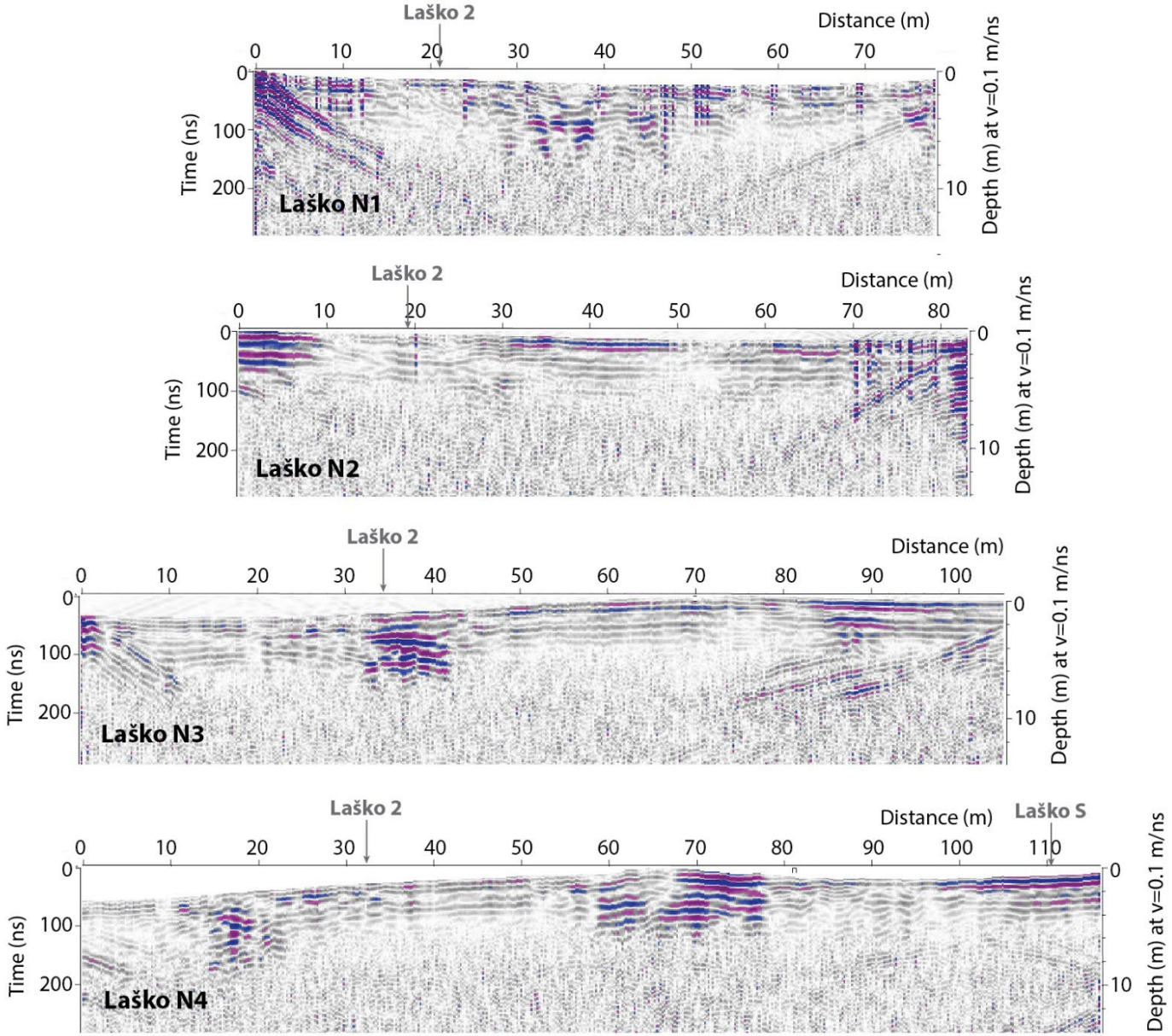

Figure S41: GPR profiles parallel to the Sava Fault at location Laško.

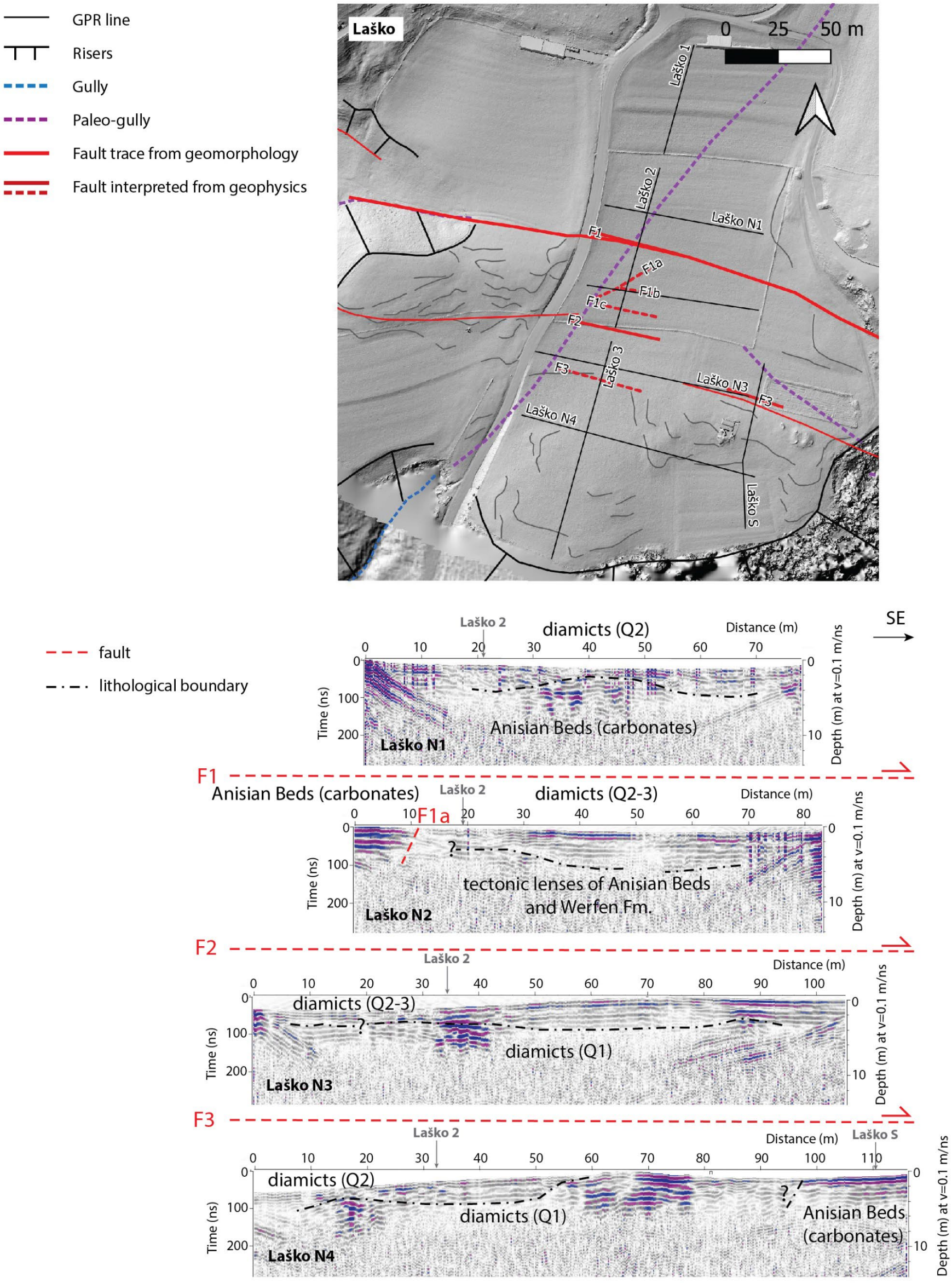

Figure S42: GPR profiles parallel to the Sava Fault at location Laško. Interpretation is based on radargram characteristics, comparison with fault perpendicular GPR and ERT profiles, tectonic geomorphological and structural-geological field mapping.

Section S5 – Luminescence Dating

This section contains the detailed description of the methodology for luminescence dating.

The sample was treated with the standard laboratory procedure (e.g., [5]) including hydrochloric acid, sodium oxalate, and hydrogen peroxide to remove carbonate, aggregates, and organic matter, respectively. After the treatments, the coarse-grained material was separated into quartz-rich ($2.62 < d < 2.7$) and K-feldspar ($d < 2.58$) fractions using heavy liquid (sodium polytungstate solution). The quartz fraction was etched using 40 % hydrofluoric (HF) acid for 1 hour to purify quartz. Unfortunately, only 20 mg of quartz remained after the HF etching, which was not sufficient for OSL measurements, whereas the separation yielded enough K-feldspar grains (~0.7 g) for infrared stimulated luminescence (IRSL) measurements. For the fine-grained fraction, ~5 g of material was separated by Stokes Law, and 2 g was used for etching with hexafluorosilicic acid for 5 days to extract quartz.

The coarse-grained K-feldspar sample was mounted on 9.8 mm diameter stainless steel discs using silicone oil spray as adhesive. The sample grains were dropped through 1 mm-size apertures on the discs, and each aliquot consists of ~10 grains. For the fine-grained quartz, the sample material was suspended in distilled water and ~2 mg each was deposited on aluminum discs. The sample for environmental dose rate measurement was dried at 110°C for 24 hours, and 50 g of the dried material was sealed in a plastic container.

Both coarse-grained K-feldspar and fine-grained quartz were used for luminescence measurements. The quartz OSL signal was detected through a 7.5 mm Hoya U-340 filter using blue LEDs (~470 nm) for stimulation. The IRSL signal was detected through a combination of Schött 7–59 and BG39 filters, which transmits violet-blue luminescence signal, stimulated by IR LEDs (~870 nm). Equivalent dose (D_e) values were measured for 18 fine-grained quartz and 24 coarse-grained K-feldspar aliquots. The measurement protocols are summarized in Table S1 [6,7]. The final D_e values for age calculation were obtained by the central age model (CAM) for quartz OSL and the minimum age model (MAM) for the K-feldspar post-IR IRSL signal at 150°C. An overdispersion parameter (s_b) of 20% was used for calculating the MAM D_e. Additionally, a dose recovery test [8] was conducted to test whether the applied protocols yield the laboratory given dose. For K-feldspar, a laboratory fading test was also performed to quantify the athermal signal loss following [9], and the age was fading-corrected using the method of [10].

The natural radioactivity of the sample was measured with an Ortec N-type pure germanium gamma detector. The activity of U, Th, and K was converted to the concentration and further to the dose rate using the conversion factors of [11].

Table S1. Luminescence measurement protocols for quartz and K-feldspar.

	Quartz OSL		**Feldspar Post-IR IRSL**	
Step	**Treatment**	**Observation**	**Treatment**	**Observation**
1	Dose		Dose	
2	Preheat 180°C, 10 s		Preheat 180°C, 60 s	
3	IRSL 125°C, 100 s		IRSL 50°C, 100 s	
4	OSL 125°C, 100 s	Lx	Post-IR IRSL 150°C, 200 s	Lx
5	Test dose		Test dose	
6	Cutheat 160°C, 0 s		Preheat 180°C, 60 s	
7	IRSL 125°C, 100 s		IRSL 50°C, 100 s	
8	OSL 125°C, 100 s	Tx	Post-IR IRSL 150°C, 200 s	Tx
9	Back to 1		Back to 1	

Supplementary Materials References:

1. Slovenian Environment Agency LIDAR Available online: http://gis.arso.gov.si/evode/profile.aspx?id=atlas_voda_Lidar@Arso (accessed on 1 March 2020).

2. Zakšek, K.; Oštir, K.; Kokalj, Ž. Sky-View Factor as a Relief Visualization Technique. *Remote Sensing 2011, Vol. 3, Pages 398-415* **2011**, *3*, 398–415, doi:10.3390/RS3020398.

3. Kokalj, Ž.; Somrak, M. Why Not a Single Image? Combining Visualizations to Facilitate Fieldwork and On-Screen Mapping. *Remote Sensing 2019, Vol. 11, Page 747* **2019**, *11*, 747, doi:10.3390/RS11070747.

4. Broglio Loriga, C.; Masetti, D., C.; Neri, C. La Formazione Di Werfen (Scitico) Delle Dolomite Occidentali: Sedimentologia e Biostratigrafia. . *Rivista Italiana di Paleontologia e Stratigrafia* **1983**, *88*, 501–598.

5. Aitken, M.J. *An Introduction to Optical Dating : The Dating of Quaternary Sediments by the Use of Photon-Stimulated Luminescence*; Oxford University Press, 1998; ISBN 0198540922.

6. Murray, A.S.; Wintle, A.G. Luminescence Dating of Quartz Using an Improved Single-Aliquot Regenerative-Dose Protocol. *Radiat Meas* **2000**, *32*, 57–73, doi:10.1016/S1350-4487(99)00253-X.

7. Reimann, T.; Tsukamoto, S. Dating the Recent Past (<500 Years) by Post-IR IRSL Feldspar – Examples from the North Sea and Baltic Sea Coast. *Quat Geochronol* **2012**, *10*, 180–187, doi:10.1016/J.QUAGEO.2012.04.011.

8. Murray, A.S.; Wintle, A.G. The Single Aliquot Regenerative Dose Protocol: Potential for Improvements in Reliability. *Radiat Meas* **2003**, *37*, 377–381, doi:10.1016/S1350-4487(03)00053-2.

9. Auclair, M.; Lamothe, M.; Huot, S. Measurement of Anomalous Fading for Feldspar IRSL Using SAR. *Radiat Meas* **2003**, *37*, 487–492, doi:10.1016/S1350-4487(03)00018-0.

10. Huntley, D.J.; Lamothe, M. Ubiquity of Anomalous Fading in K-Feldspars and the Measurement and Correction for It in Optical Dating. *Can J Earth Sci* **2001**, *38*, 1093–1106, doi:10.1139/E01-013.

11. Liritzis, I.; Stamoulis, K.; Papachristodoulou, C.; Ioannides, K. A Re-Evaluation of Radiation Dose-Rate Conversion Factors. *Mediterranean Archaeology and Archaeometry* **2013**, *13*, 1–15.